The tonalite–trondhjemite–granodiorite (TTG) to granodiorite–granite (GG) transition in the late Archean plutonic rocks of the central Wyoming Province[1]

Carol D. Frost, B. Ronald Frost, Robert Kirkwood, and Kevin R. Chamberlain

Abstract: The 2.95–2.82 Ga quartzofeldspathic gneisses and granitoids in the Bighorn, western Owl Creek, and northeastern Wind River uplifts in the central Wyoming Province include low-K tonalite–trondhjemite–granodiorite (TTG) and high-K granodiorite–granite (GG) rocks. Both types of granitoids were intruded contemporaneously, although TTGs are more abundant in the older gneisses. The TTG suite consists of calcic to marginally calc-alkalic rocks that straddle the boundaries between metaluminous and peraluminous and between ferroan and magnesian compositions. Rare-earth element (REE) patterns of these rocks may be highly fractionated with low heavy rare-earth element (HREE) contents and modest to absent Eu anomalies but may also be less strongly HREE depleted. These rocks do not represent first-generation continental crust: most have unradiogenic Nd and radiogenic $^{207}Pb/^{204}Pb$ isotopic compositions that require the incorporation of isotopically evolved sources. The GG suite has compositions that are transitional between Archean TTG and modern, continental margin calc-alkalic rocks. The GG suite is characterized by higher alkali contents relative to CaO than the TTG suite and higher K/Na ratios but exhibits a similar range in REE patterns. The Nd, Sr, and Pb isotopic compositions of the GG suite are slightly less variable but lie within the range of those of the TTG suite. We interpret them as having a source similar to that of the TTG, perhaps forming by partial melting of preexisting TTG. The shift from TTG-dominated to GG-dominated continental crust was a gradual transition that took place over several hundred million years. Clearly subduction-related calc-alkalic magmatism is not recognized in the Wyoming Province prior to 2.67 Ga.

Résumé : Les gneiss et les granitoïdes quartzo-feldspathiques, 2,95 – 2,82 Ga, dans les soulèvements de Bighorn, de l'ouest d'Owl Creek et du nord-est de Wind River dans le centre de la Province de Wyoming comprennent des roches tonalite–trondhjémite–granodiorite (TTG) à faible teneur en K et des roches granodiorite–granite (GG) à teneur élevée en K. Les deux types de granitoïdes ont été pénétrés en même temps, bien que les roches TTG soient plus abondantes dans les gneiss plus anciens. La suite TTG comprend des roches calciques à légèrement calco-alcalines qui chevauchent les limites entre les compositions métalumineuses et hyperalumineuses et les compositions ferrifères et magnésiennes. Les patrons des éléments des terres rares de ces roches peuvent être hautement fractionnés avec une faible teneur en éléments des terres rares lourdes et des anomalies Eu modestes à absentes, mais les roches peuvent aussi être moins appauvries en éléments des terres rares lourdes. Ces roches ne représentent pas une croûte continentale de première génération : la plupart ont des compositions isotopiques Nd non radiogéniques et des compositions $^{207}Pb/^{204}Pb$ radiogéniques qui demandent l'incorporation de sources isotopiquement évoluées. La suite de roches GG possède des compositions qui représentent une transition entre des roches TTG archéennes et des roches calco-alcalines et modernes de bordure continentale. La suite GG est caractérisée par une teneur plus élevée en alcalins, relativement au CaO, que la suite de roches TTG et des rapports K/Na supérieurs, mais elle présente une plage semblable de patrons d'éléments des terres rares. Les compostions isotopiques Nd, Sr et Pb de la suite GG varient un peu moins mais elles se trouvent à l'intérieur de la plage de la suite TTG. Nous suggérons qu'elles aient la même source que la suite TTG, s'étant possiblement formées par la fusion partielle d'une suite TTG préexistante. Le passage d'une croûte continentale dominée par des roches TTG à une suite dominée par des roches GG s'est effectué par une transition graduelle sur plusieurs centaines de millions d'années. Un magmatisme calco-alcalin clairement relié à la subduction n'est pas reconnu dans la Province de Wyoming avant 2,67 Ga.

[Traduit par la Rédaction]

C.D. Frost,[2] B.R. Frost, R. Kirkwood, and K.R. Chamberlain. Department of Geology and Geophysics, University of Wyoming, Laramie, WY 82071, USA.

[1]This paper is one of a selection of papers published in this Special Issue on *The Wyoming Province: a distinctive Archean craton in Laurentian North America.*
[2]Corresponding author (e-mail: frost@uwyo.edu).

Introduction

Gray gneisses of tonalite–trondhjemite–granodiorite (TTG) affinity make up much of the basement in Archean provinces worldwide; consequently, an understanding of their petrogenesis provides important insights into early crust-forming processes. These rocks, estimated by Martin et al. (2005) to make up around 90% of Archean-age juvenile continental crust, typically are composed of quartz, plagioclase, and biotite, and locally also contain hornblende. They are silica rich, with SiO_2 contents of around 70 wt.%, and have high Na_2O (>3.0 wt.%) and high Al_2O_3 (>15.0 wt.%). Archean TTGs are characterized by steep negative rare-earth element (REE) patterns and low heavy rare-earth element (HREE) contents (Barker and Arth 1976; Jahn et al. 1981; Martin 1994; Martin et al. 2005). Many TTGs have mantle-like isotopic compositions, although there is some variability. It is not clear if the variations reflect mantle heterogeneity or involvement of crustal sources (Martin 1994). Most recent models interpret these features as the result of partial melting of a tholeiitic source in which garnet and amphibole are residual phases, although the tectonic settings in which the tholeiite is formed and subsequently partially melted remain the subject of debate (e.g., Martin and Moyen 2002; Smithies et al. 2003).

A substantial portion of the central Wyoming Province is composed of TTG gneisses that range in age from ≥2.95 to 2.80 Ga. For the most part, the rocks have not been deformed or metamorphosed since 2.80 Ga, and therefore these exposures represent an important opportunity to unravel their field relations, geochemistry, and petrogenesis. In addition, the Wyoming Province TTGs are relatively late: when these rocks formed in the late Archean, crustal and depleted mantle reservoirs had evolved isotopically to distinct compositions. For this reason, a study of these rocks represents a better opportunity to evaluate the age and origin of the sources of TTG magmas than do studies of much older TTG terrains.

A notable feature of the central Wyoming Province is that a suite of high-K granodiorite–granite (GG) rocks also occurs together with those of TTG affinity. The youngest of these GG suites occur in elongate belts parallel to the margin of the province and are interpreted as late Archean subduction-related continental margin magmatism (Frost et al. 1998). Other, older high-K granodiorites and granites appear to be coeval with the TTG rocks, and as such represent an opportunity to investigate the relationship between TTG and high-K granitoids.

Archean geology of the Wyoming Province

In the Wyoming Province, Archean rocks are extensively exposed in the Laramide (Cretaceous) basement-cored uplifts of the Rocky Mountain foreland (Fig. 1). These uplifts provide an important window in the Archean crust that underlies much of Wyoming and parts of adjacent states of South Dakota, Montana, Idaho, Utah, and Nevada. Some of the oldest rocks in the province include igneous rocks of low-K TTG and high-K GG affinity, which occur in the Eastern Beartooth Mountains and the Bighorn Mountains of northern Wyoming and adjacent parts of Montana, with smaller exposures in the western Owl Creek Mountains and northeastern Wind River Range. Mogk et al. (1992) and Mueller et al.

(1996) referred to the area occupied by these rocks as the Beartooth–Bighorn magmatic zone (BBMZ). The Archean geology of the Beartooth Mountains has been described by Wooden and Mueller (1988), Mueller et al. (1988), Wooden et al. (1988), and Mogk et al. (1992). In this paper we describe the Archean rocks of the Bighorn Mountains, western Owl Creek Mountains, and Washakie block of the northeastern Wind River Range (Figs. 2–4).

Geology of the Bighorn uplift

The Archean rocks of the Bighorn uplift can be divided into a central and southern area of quartzofeldspathic gneiss and minor supracrustal rocks intruded in the northern part of the uplift by an undeformed granitoid batholith (Fig. 2).

Central and southern gneiss terrain

The central and southern gneiss terrain of the Bighorn Mountains is composed of plagioclase–quartz gneiss, including biotite-rich and hornblende-rich varieties. Most common is mafic-poor, plagioclase–quartz gneiss. Typically equigranular, the gneisses are characterized locally by the presence of feldspar augen. Most gneisses are layered on a scale of centimetres to metres. Layers can be traced for up to 10 m; they may pinch and swell or grade into more massive gneiss. Interlayered with the gneiss is amphibolite and locally quartzite and schist. The amphibolite bodies vary in thickness from 15 cm to 60 m, although the map-scale supracrustal belt south of Highway 16 at Hazelton Peak includes amphibolite up to 760 m in thickness (Heimlich et al. 1972). Another distinctive area of supracrustal rocks is present in the Horn area of the southeastern central gneiss terrain. This area exhibits the greatest variety of lithologies, including garnetiferous gneiss, amphibolite, banded iron formation, marble, and quartzite (Palmquist 1965). On the basis of detailed mapping in the Lake Helen quadrangle, Barker (1982) identified two major groups of gneisses: an older, foliated and layered quartzofeldspathic gneiss with minor lenses and interlayers of amphibolite that he called E-1 gneisses; and a younger granitic intrusive complex consisting of variably deformed granite, granodiorite, quartz diorite, and tonalite gneiss and essentially undeformed crosscutting, leucocratic dikes that he called E-2 gneisses. The younger E-2 rocks include a unit identified as the Lake McLain quartz diorite by Heimlich (1969). Farther south, Wells (1975, 1977) described a quartzofeldspathic gneiss interlayered with amphibolite and biotite gneiss and identified two folding events. These gneisses appear mineralogically and geochemically similar to the gneisses in the central Bighorn Mountains (this study).

The modal abundances of quartz, plagioclase, and microcline of 120 samples of gneiss from the central gneiss terrain indicate that the vast majority are tonalites (85), with fewer granodiorites (28) and sparse granites (7; Heimlich et al. 1972). Modal abundances of samples from Heimlich et al. (1972) for which chemical analyses are also available are plotted in Fig. 5, along with his average modal compositions for gneiss, augen gneiss, and quartz diorite units that he distinguished in the central gneiss terrain (Heimlich 1969, 1971).

A number of units from the central gneiss terrain are well dated: a diorite sill within layered gneiss yielded a U–Pb

Fig. 1. Map showing the location of Precambrian-cored Laramide-age uplifts in the Wyoming Province. Archean rocks lie north of the Cheyenne Belt (CB) and southeast of the Great Falls tectonic zone (GFTZ). N MR, North Madison Range; S MR, South Madison Range; TR, Tobacco Root Mountains. Inset shows location of the Wyoming Province (WP) with respect to the Superior Province (SP) and Proterozoic rocks (P) to the south.
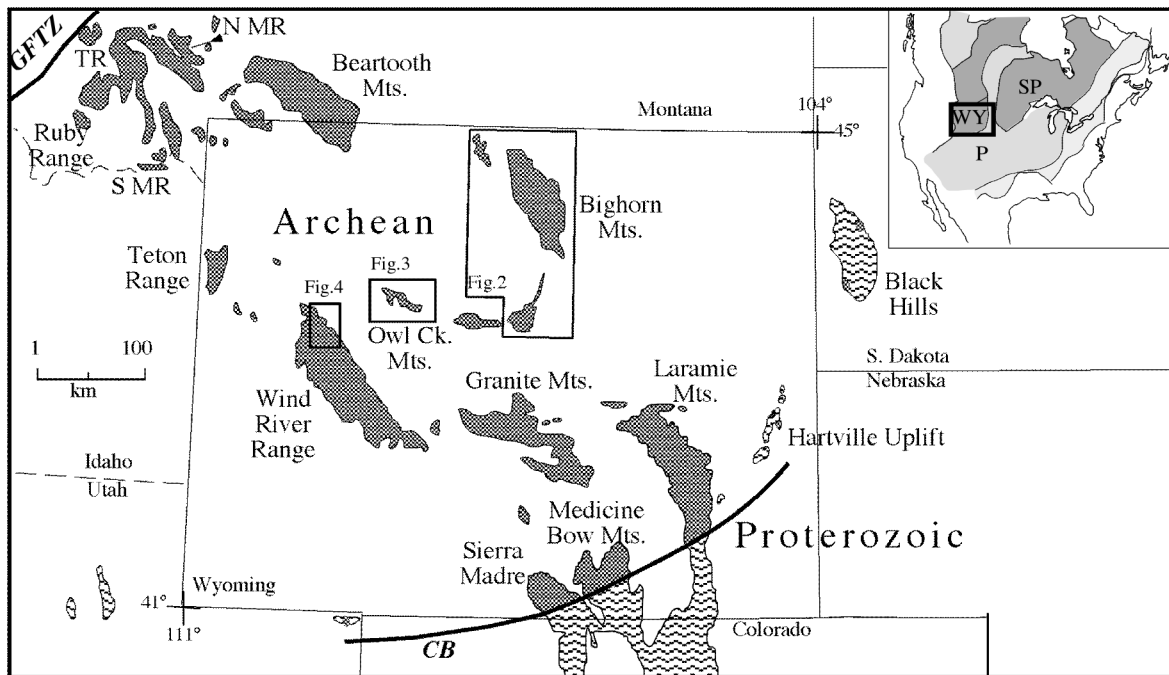
zircon sensitive high-resolution ion microprobe (SHRIMP) date of 2952 ± 4 Ma, and a granodiorite dike within the supracrustal sequence at Hazelton Peak was intruded at 2949 ± 5 Ma (Frost and Fanning 2006). A layered tonalite gneiss from the E-1 gneisses of Barker (1982) is somewhat younger, at 2886 ± 5 Ma. This tonalite yielded some zircon domains with ^{207}Pb/^{206}Pb ages as old as 3.00 Ga, suggesting the incorporation of zircon from older crust or from sedimentary rocks with old detrital components. A sample of E-2 gneiss yielded a group of concordant U–Pb zircon data of 2937 ± 5 Ma. The oldest ^{207}Pb/^{206}Pb ages obtained from cores and centers of zircon crystals from this sample are ca. 3.25 Ga. Gneiss from the southern gneiss terrain also appears to be approximately 2.90 Ga (Frost and Fanning 2006). On the basis of this geochronology, it appears that the gneiss terrain is made up of rocks that are ≥2.95 Ga in age and continued to be intruded by tonalitic magmas until at least 2.89 Ga. Deformation event(s) then produced the strong foliation in these rocks prior to the intrusion of the Bighorn batholith between 2.86 and 2.84 Ga (Frost and Fanning 2006).
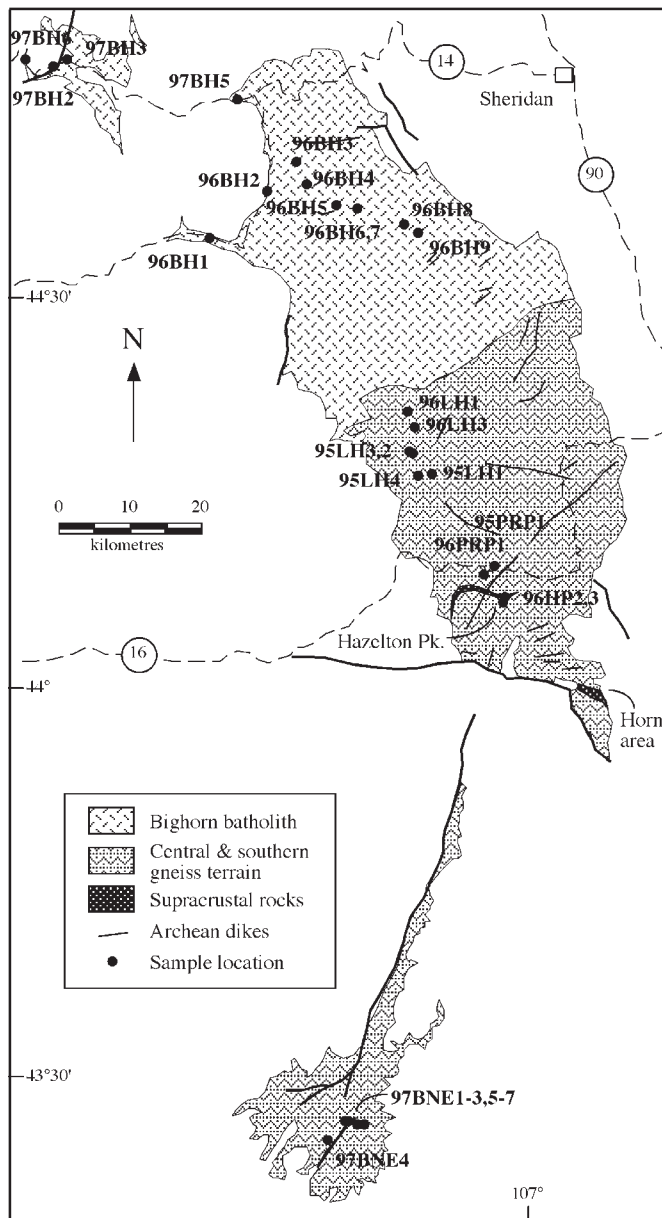
Bighorn batholith

The undeformed granitic rocks in the northern Bighorn Mountains are referred to in this study as the Bighorn batholith. Darton (1906) first described these granitoids, recognizing a coarse-grained red lithology that is most common in the northwestern part of the uplift and a medium gray lithology that dominates the outcrop in the southern part of the batholith. Modal mineralogy of these two groups of granitoids determined by Heimlich (1969, 1971) and this study (Table 1) indicates that the red unit is mainly granite sensu stricto that is locally quartz monzonite and the gray unit is granodiorite

to tonalite in composition (Fig. 5). Both rock types are composed of microcline, quartz, and plagioclase in varying proportions, with accessory biotite, hornblende, Fe–Ti oxides, titanite, zircon, and allanite, with secondary chlorite and epidote. Sulfides are present locally. A sample of the red granite has been dated at 2859 ± 3 Ma, and a gray granodiorite sample at 2844 ± 5 Ma (Frost and Fanning 2006). Both samples yielded zircon analyses with slightly older ^{207}Pb/^{206}Pb ages (as old as 2.94 Ga) that are interpreted to represent inherited components. Along the southern margin of the batholith is an area in which metre-sized blocks, ovoidal lenses, and irregularly shaped fragments of tonalitic gneiss are enclosed by biotite granite and granodiorite. This unit was described as agmatite by Heimlich (1969) and Barker (1982), and we interpret it as an intrusive breccia along the contact of the batholith with the central gneiss terrain.

Late intrusions

Tholeiitic mafic dikes, including a suite of plagioclase porphyry dikes (Heimlich and Manzer 1973), crosscut the Bighorn batholith and the central gneiss terrain. Mafic dikes also are present, though uncommon, in the southern portion of the gneiss terrain (Houston et al. 1993). Stueber et al. (1976) and Armbrustmacher (1972) have identified two generations of dikes, dated by Rb–Sr whole rock and mineral isochrons at 2.77 ± 0.12 and 2.15 ± 0.20 Ga. The gneisses in the southern Bighorn Mountains are intruded locally by garnet-bearing granite. These are undated but may be part of a suite of volumetrically minor but widespread garnet granites that occur within the 2.62 Ga Granite Mountains batholith (Stuckless and Miesch 1981).

Fig. 2. Geological sketch map of the Archean rocks of the Bighorn Mountains, indicating major Archean units, Precambrian mafic dikes, and sample locations. Sample names containing LH are from the Lake Helen quadrangle mapped by Barker (1982).

Hornblende tonalite gneiss, which contains sodic hornblende and minor biotite, is coarse grained and slightly foliated. Hornblende tonalite gneiss grades into biotite tonalite gneiss, which has a strong migmatitic texture. Granodiorite gneiss occurs both as layered migmatitic gneiss and as slightly foliated plutons intruding hornblende tonalite gneiss. Granite gneiss forms small pods throughout the western Owl Creek Mountains. It is fine grained and strongly foliated. The gneisses have been metamorphosed at amphibolite facies but contain relict tabular plagioclase indicative of their igneous origin. Locally the gneisses are cut by millimetre-wide greenschist-grade deformation zones.

Kirkwood (2000) obtained U–Pb zircon thermal ionization mass spectrometry (TIMS) dates on four samples of quartzofeldspathic gneiss. The hornblende, biotite, and granodiorite gneisses yielded the same age within analytical uncertainty: 2842 ± 2, 2843 ± 6, and 2837 ± 4 Ma, respectively. A second population of zircon in the hornblende tonalite gneiss gave a younger age of 2824 ± 3 Ma, which has been interpreted as either the best estimate of the crystallization age of the gneiss or the time of metamorphic zircon growth related to slightly younger intrusive events (Kirkwood 2000). A younger period of magmatism in the western Owl Creek Mountains is suggested by the preliminary age of 2815 ± 2 Ma from a second granodiorite gneiss sample, which is based on a single concordant analysis of zircon. Evidence of an inherited zircon component in this granodiorite sample is suggested by slightly older $^{207}Pb/^{206}Pb$ ages of a few abraded zircon fractions (Kirkwood 2000).

Associated with these felsic gneisses are minor occurrences of supracrustal rocks. The most abundant is garnet–cordierite schist; in addition, a single outcrop of iron formation was identified, as was a calc-silicate mylonite (Kirkwood 2000).

The mafic to ultramafic dike swarm, which trends northwest–southeast, includes peridotite, gabbro, and plagioclase porphyry dikes. The plagioclase porphyry dikes are similar in appearance to those in the Bighorn Mountains. The dikes are undeformed and unmetamorphosed except for greenschist-grade veins of quartz, epidote, and actinolite. A gabbroic dike has been dated by the U–Pb method on baddeleyite at 2680 ± 4 Ma (Kirkwood 2000; Frost et al. 2006). Like the Bighorn Mountains, the western Owl Creek Mountains have not experienced the later Archean magmatic, metamorphic, and deformation events that dominate the southern and western Wyoming Province (Frost et al. 1998; Chamberlain et al. 2003).

Washakie block

The Washakie block is an area of quartzofeldspathic gneisses in the northeast portion of the Wind River Range that preserve a record of the earliest events in the uplift (Fig. 4) (Frost et al. 1998; Frost et al. 2000). The block lies on the hanging wall of the Mount Helen structural zone (MHSZ). It is bounded on the southwest by the MHSZ, on the north by migmatites of the 2.67 Ga Bridger batholith (Aleinikoff et al. 1989), and on the south by the 2.63 Ga Louis Lake batholith (Frost et al. 1998). Locally, gneisses contain foliations that are parallel to the northwest–southeast trend of the MHSZ and have been interpreted to record metamorphism and deformation at ca. 2.67 Ga (Frost et al. 2000). Granodiorite dikes, presumably of Bridger age, also intrude the gneisses of the Washakie block. The Bridger dikes form a minor

Western Owl Creek Mountains

The Owl Creek Mountains, a small east–west-oriented Laramide uplift that lies south and west of the Bighorn Mountains, are divided into two parts by the Wind River Canyon. The Archean rocks in the eastern Owl Creek Mountains consist of a ca. 2.90 Ga supracrustal belt that has been intruded by 2.60 Ga peraluminous granite (Hausel 1985; Mueller et al. 1985; Hedge et al. 1986; Stuckless et al. 1986). The Archean rocks in the western Owl Creek Mountains consist of quartzofeldspathic gneisses that have been intruded by a mafic dike swarm (Fig. 3).

Four different units within the gneiss complex in the western Owl Creek Mountains have been identified (Kirkwood 2000).

Fig. 3. Sketch map of the Archean rocks of the western Owl Creek Mountains from Kirkwood (2000), showing major units and sample locations.
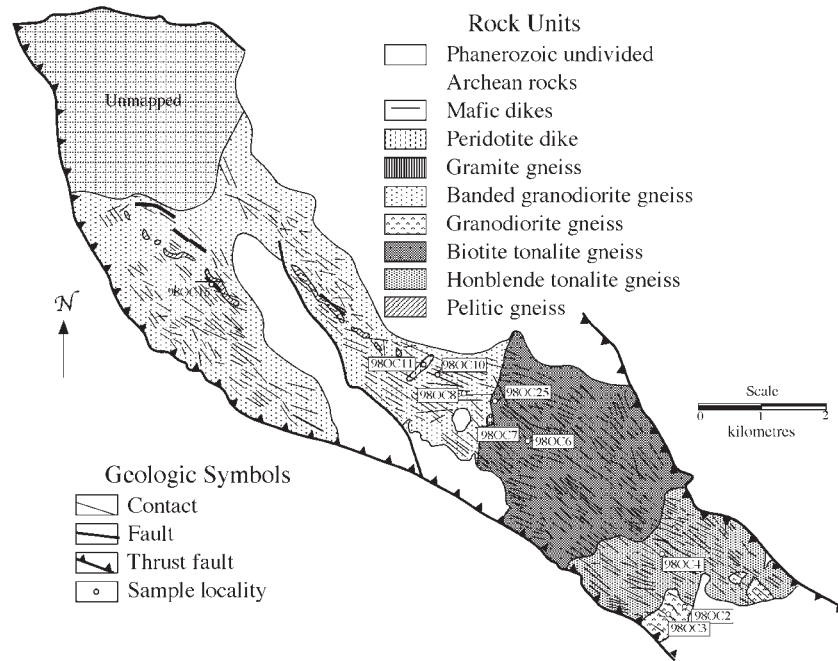
component of the gneisses throughout most of the Washakie block but become more abundant to the north until they make up more than 50% of the outcrop. Exposures of the Washakie gneisses ultimately are obliterated by migmatites that form the eastern margin of the Bridger batholith.

The gneisses of the Washakie block are dominated by layered gray gneisses. These are typically strongly foliated and are folded with supracrustal enclaves composed of metaperidotite, metabasalt, sulfidic metaquartzite, semipelitic gneiss, and minor calc-silicate gneiss and iron formation. Individual outcrops of supracrustal rocks are up to several hundred metres wide and extend from 100 m to 1 km in length. The common metamorphic grade for these supracrustal rocks is amphibolite facies, but traces of earlier granulite metamorphism are found locally (Frost et al. 2000). The layered gray gneisses are composed of plagioclase, quartz, and biotite ± hornblende, with accessory titanite, allanite, and zircon. They display an intense north–south-striking foliation. Frost et al. (1998) reported a preliminary U–Pb age for a sample of layered gneiss of ~2.80 Ga; this date has been refined by U–Pb SHRIMP dates on two additional samples of 2843 ± 4 and 2843 ± 6 Ma. Both of these samples include a population of older zircon of approximately 2.89 Ga that is interpreted as inherited from preexisting crust (K.R. Chamberlain, B.R. Frost, and C.M. Fanning, unpublished data, 2000).

A distinctive rock unit in the Washakie block is a gray granodiorite that has a spotted texture produced by clots of biotite and hornblende. The biotite and hornblende clots in this unit, which we call the Native Lake gneiss, appear to be products of subsolidus hydration of orthopyroxene, indicating that the gneiss was originally crystallized as a charnockite. Only locally does the Native Lake gneiss retain the primary pyroxene. The Native Lake gneiss crops out as homogeneous exposures with areal extents of several hundred square metres in several places throughout the Washakie block. It also occurs as a narrow layer on the footwall of the MHSZ between the

MHSZ and the Bridger batholith. In some places it intrudes layered gray gneiss, but in most areas the Native Lake gneiss is found within complex migmatitic orthogneiss. One sample of Native Lake gneiss dated using the U–Pb SHRIMP method on zircon yielded an age of 2866 ± 5 Ma, with no indication of inherited zircon (K.R. Chamberlain, B.R. Frost, and C.M. Fanning, unpublished data, 2000). Precambrian mafic dikes intrude the gneisses of the Washakie block. One tholeiitic dike has been dated at 2.68 Ga (Frost et al. 2006).

In summary, the Bighorn, western Owl Creek, and northeastern Wind River uplifts have similar geologic histories. These areas expose tonalitic to granitic orthogneisses that are intruded by granite and granodiorite plutons. The oldest rocks that have been dated are located in the central Bighorn Mountains, where 2.95 Ga dikes and sills intrude older gneisses. All three uplifts expose gneisses and intrusions that range in age from 2.87 to 2.82 Ma; these make up most of the exposed crust in the northern Bighorn Mountains, western Owl Creek Mountains, and Washakie block. Mafic dike emplacement occurred at 2.68 Ga in the western Owl Creek Mountains and in the Washakie block; the ages of similar mafic dikes in the Bighorn Mountains are less well known but are the same within analytical uncertainty.

Geochemistry

Major elements

Major element geochemistry for Bighorn Mountain gneisses and the Bighorn batholith (Table 2) and for the Owl Creek Mountains and Washakie block gneisses (Table 3) indicates that the rocks from these uplifts span the compositional range from tonalite to granite. Most of the quartzofeldspathic gneisses studied here are calcic according to the modified alkali-lime index of Frost et al. (2001) (Fig. 6A). The rocks of the Bighorn batholith, in contrast, are mainly calc-alkalic, and two granite samples from the western Owl Creek Moun-

Fig. 4. Geological map of the Archean rocks of the Washakie block, northeastern Wind River Range. Several gneissic units, mapped as Native Lake gneiss, layered gray gneiss, and mixed gneiss, are intruded by the 2.67 Ga Bridger batholith and Bridger migmatite. The Mount Helen structural zone is a southwest-vergent ductile thrust that was active around 2.70–2.67 Ga (Frost et al. 2000).
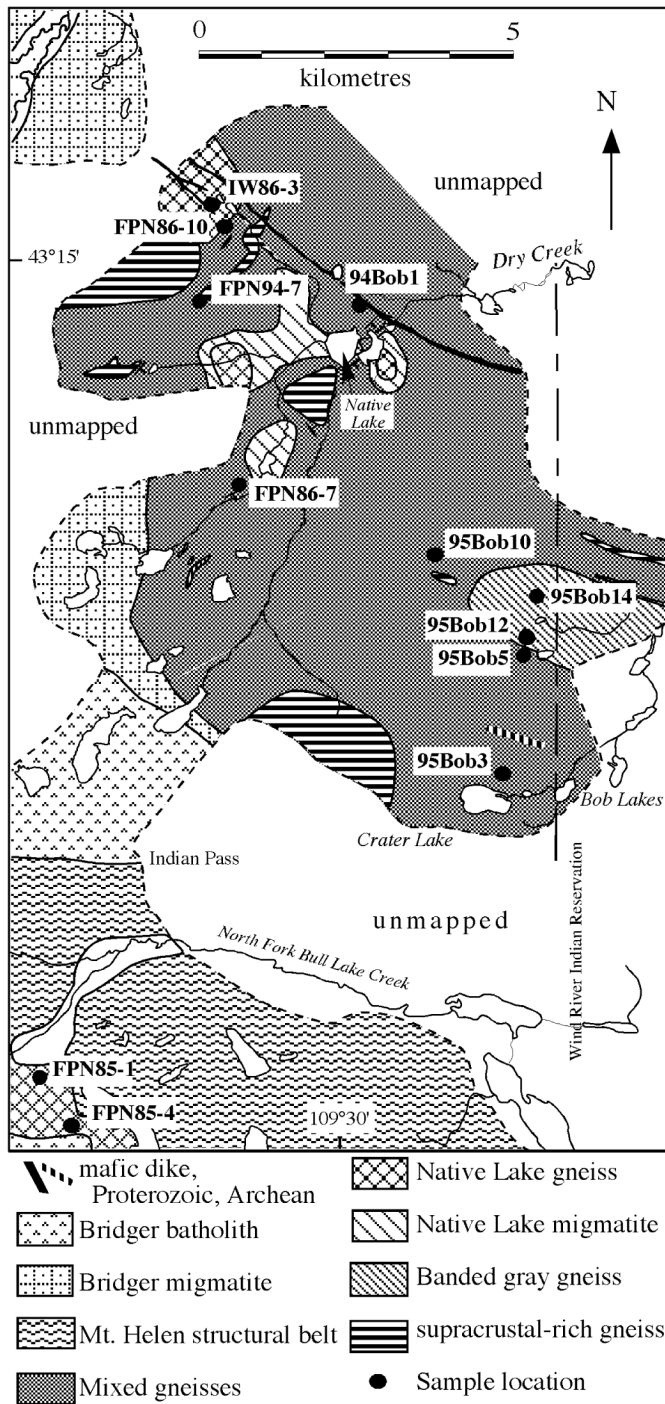
Fig. 5. Modal compositions of granitoid rocks from the Bighorn batholith, Bighorn gneiss terrain, and western Owl Creek Mountains. Average modal compositions of gneisses from the central gneiss terrain and granitoids from the Bighorn batholith compiled by Heimlich (1969) are shown by circles with vertical rules and squares with vertical rules, respectively. Other data for individual samples are from Table 1 and Heimlich (1971). A, alkali feldspar; P, plagioclase; Q, quartz.
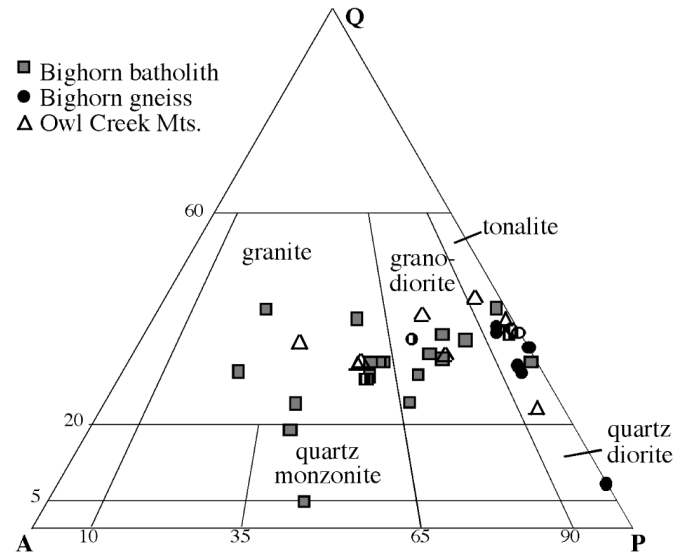
related magmatic suites and Archean tonalite suites worldwide (Frost et al. 2001). A notable feature of the Wyoming Province 3.00–2.80 Ga felsic gneisses and granitoids is that they are mainly peraluminous (Fig. 6C).

The sodium contents of the granitoids vary greatly, from less than 3 wt.% Na_2O to almost 6 wt.% (Fig. 7A), and K_2O for most samples is in the medium- to high-K range (Fig. 7B). A number of the Bighorn gneisses, characterized by SiO_2 around 70%, have high Na_2O contents around 5%; this combined with their low K_2O contents (Fig. 7B) leads to Na_2O/K_2O greater than 3 (Fig. 7C). These same Bighorn gneiss samples also have higher Al_2O_3 than rocks with comparable SiO_2 contents from the Bighorn batholith, Washakie block, and western Owl Creek Mountains (Fig. 8).

Trace elements

Many Archean TTG suites are characterized by high Sr contents, typically greater than 400 ppm (Martin et al. 2005). Although the Sr contents of some of the quartzofeldspathic gneisses and granitoids of this study exceed 400 ppm, Sr contents are variable (from 134 to 553 ppm, plus one additional sample with 671 ppm), and 85% of our samples have Sr lower than 400 ppm (Fig. 9). The low Sr contents may reflect late-stage plagioclase fractionation in the Wyoming Province TTG suite.

Samples from each of the study areas exhibit significant variations in REE patterns, both in terms of pattern steepness and size of the europium anomaly (Fig. 10). For example, $(La/Yb)_N$ for granitoids and gneisses from the Bighorns varies from 8 to 107, and europium anomalies vary from positive (Eu/Eu* = 2.3) to negative (Eu/Eu* = 0.63). Although fewer data are available from the Washakie block and western Owl

tains are alkali-calcic. Most of the gneisses and Bighorn batholith samples are magnesian (Fig. 6B), although a subset of the most siliceous samples is ferron. The trend from magnesian to ferron compositions is a feature of subduction-

Table 1. Modal percentages of alkali feldspar (A), plagioclase (P), and quartz (Q) determined for representative samples of the Bighorn batholith and the western Owl Creek Mountains.

Sample No.	A	P	Q
Bighorn batholith			
96BH1	0.25	0.43	0.32
96BH2	0.48	0.34	0.19
96BH3	0.26	0.42	0.32
96BH4	0.13	0.50	0.37
96BH5	0.27	0.44	0.29
96BH6	0.24	0.44	0.32
96BH8	0.15	0.52	0.33
96BH9	0.09	0.54	0.36
97BH1	0.50	0.20	0.30
97BH2	0.40	0.18	0.42
97BH3	0.16	0.50	0.34
97BH4	0.52	0.43	0.05
97BH5	0.21	0.50	0.29
97BH6	0.25	0.51	0.24
Western Owl Creek Mountains			
98OC2	0.15	0.52	0.33
98OC4	0.05	0.73	0.22
98OC6	0.05	0.52	0.43
98OC7	0.38	0.27	0.35
98OC8	0.15	0.45	0.40
98OC19	0.30	0.39	0.31
98OC20	0.02	0.59	0.39
98OC21	0.28	0.40	0.32

Note: Modal proportions were determined from stained slabs, and a minimum of 700 points counted.

Creek gneisses, they also exhibit similarly variable patterns, ranging from light rare-earth element (LREE) enriched patterns with negative Eu anomalies similar to those of calc-alkalic rocks to patterns with extreme HREE depletion and slightly positive to absent Eu anomalies like those of many Archean TTG suites (Figs. 10D, 10E). The samples with high $(La/Yb)_N$ are not restricted to tonalites and trondhjemites, but include granites. Conversely, the samples with fewer HREE-depleted patterns and negative europium anomalies include tonalites, granodiorites, and granites. The 2.63 Ga, calc-alkalic Louis Lake batholith in the central Wind River Range shows a variation in REE patterns similar to that of the older rock suites (Fig. 10F). Among the older granitoids there is a weak correlation of increasing $(La/Lu)_N$ with increasing SiO_2 and Fe* such that REE patterns are flattest for the samples with lowest silica, but the most siliceous samples exhibit a range of $(La/Lu)_N$ (Fig. 11).

Comparison with Archean TTG suites

Key geochemical features of Archean TTG suites include high SiO_2, commonly ~70 wt.% or greater, high Na_2O (>3.0 wt.%), and high Na_2O/K_2O (>2). Among these suites, Barker and Arth (1976) recognized two groups: a high-Al group (Al_2O_3 > 15 wt.%) with elevated Sr and strongly fractionated REE patterns ($(La/Yb)_N$ up to 150), and a low-Al group (Al_2O_3 < 15 wt.%) with lower Sr and less fractionated REE. The former was interpreted as reflecting a petrogenesis in which garnet was a residual or fractionating phase, and the latter in which plagioclase was present rather than garnet.

Compared with average compositions for TTG rocks of varying ages (>3.50, 3.50–3.00, and <3.00 Ga; Martin et al. 2005), the gneisses of this study are similarly calcic to marginally calc-alkalic and magnesian but slightly more siliceous (cf. Figs. 6A, 6B). Average TTG have alumina saturation indices near 1, whereas Wyoming gneisses are somewhat more peraluminous, particularly the samples from the Washakie block.

A subset of samples from all three uplifts shares the diagnostic Na_2O contents and Na_2O/K_2O ratios of Archean TTG. They are characterized by low K_2O and by Na_2O between 5 and 6 wt.%, which in turn produces Na_2O/K_2O of 3–5 (Figs. 7A–7C). These "sodic" samples also have the high Al_2O_3 that typifies the high-Al group of Archean TTG (Fig. 8). Many of the sodic samples are from the central gneiss terrain of the Bighorn Mountains, but they are not restricted to a single intrusion or particular geographic area within that terrain. Moreover, samples with similar compositions are located in the Bighorn batholith and in the western Owl Creek and Wind River uplifts.

A majority of the samples in our dataset are more potassic and less sodic than the typical TTG. Most granitoids from the Bighorn batholith are high K_2O (Fig. 7B) and have Na_2O contents between 3 and 4 wt.% (Fig. 7A). A number of samples from the Bighorn, Owl Creek, and Wind River uplifts also share these characteristics. The Sr contents of most of the Wyoming gneisses and granitoids are lower than average values for Archean TTG (454–435 ppm; Martin 1994; Condie 1993). We conclude that the BBMZ is composed of rocks of both TTG affinity and high-K GG association. Although a greater proportion of tonalitic rocks is present in the oldest gneisses, such as those preserved in the Bighorn Mountains, high-K granitic and tonalitic rocks occur together spatially and temporally in all of the study areas.

Nd, Sr, and Pb isotopic compositions

Published isotopic data on the ca. 3.00–2.80 Ga quartzofeldspathic rocks of the BBMZ are limited to Sr, Nd, and Pb isotopic compositions for rocks from the eastern Beartooth Mountains (Wooden and Mueller 1988) and five Pb and seven Nd and Sr isotopic analyses of gneisses from the Washakie block (Frost et al. 1998). As part of this study, we obtained additional Rb–Sr and Sm–Nd isotopic data for five samples from the Washakie block along with eight samples from the western Owl Creek Mountains and 30 samples from the Bighorn Mountains. In addition, we present Pb isotopic data on four step-dissolved feldspars from the western Owl Creek Mountains and U–Pb whole rock data on 28 samples from the Bighorn Mountains. These data, along with analytical details, are reported in Tables 4–6.

The ca. 2.95 Ga gneisses from the central and southern Bighorn Mountains have initial ε_{Nd} that range from contemporary depleted mantle compositions of +3.7 (depleted mantle model of Goldstein et al. 1984) to –3.6, with one additional analysis of –9.9 (Table 4). There is a slight suggestion of

Table 2 (*runs from p. 1426 to p. 1429*) Geochemical data for Archean rocks of the Bighorn Mountains.

	Gneisses from the central and southern Bighorn Mountains							
Sample No.:	95LH1	95LH2	95LH3	95LH4	95PRP1	96HP2	96HP3	96LH1
Description:[a]	QFG	QFG	QFG	QFG	QFG	QFG	A	QFG
SiO_2 (wt.%)	70.7	66.6	71.9	72.1	61.8	66.6	49.4	66.3
TiO_2	0.26	0.59	0.28	0.14	0.72	0.48	0.87	0.74
Al_2O_3	15.8	15.8	14.7	15.0	16.5	16.1	13.9	16.1
FeO^t	1.86	3.97	1.81	1.10	5.38	3.12	11.34	4.28
MnO	0.02	0.04	0.02	0.01	0.07	0.05	0.18	0.05
MgO	0.74	1.45	0.57	0.28	2.07	1.54	7.93	1.68
CaO	3.17	3.80	2.27	2.59	4.82	4.23	11.00	4.38
Na_2O	4.98	4.24	4.18	4.13	4.05	5.24	1.60	3.99
K_2O	1.26	1.66	3.03	2.67	1.84	0.07	0.16	1.42
P_2O_5	0.08	0.18	0.08	0.04	0.19	0.11	0.06	0.19
LOI	0.25	0.20	0.40	0.30	0.70	0.25	0.50	0.30
Total	99.12	98.52	99.24	98.36	98.14	97.80	96.94	99.43
A/CNK	1.03	1.01	1.03	1.04	0.95	0.98	0.61	1.00
Fe^*	0.72	0.73	0.76	0.80	0.72	0.67	0.59	0.72
MALI	3.07	2.1	4.94	4.21	1.07	1.08	−9.24	1.03
Rb (ppm)	45	67	107	44	70		6	72
Sr	421	336	221	377	401	191	108	359
Zr	134	261	191	117	186	155	51	173
Y	16	20	27	16	18	18	23	14
Nb	6	10	14	5	7	5	10	7
Ba	375	746	763	1960	488	199	68	567
La	24.4			10.0	15.7	15.9	2.7	49.3
Ce	44.5			21.0	32.0	29.0	7.0	91.1
Nd	16.3			5.8	15.0	13.0	5.0	35.7
Sm	2.80			1.10	3.10	2.04	1.86	6.00
Eu	0.79			0.75	0.96	0.81	0.79	1.67
Gd	2.2			0.9				5.0
Tb	0.3			0.1	0.4	0.2	0.4	0.7
Dy	1.2			0.6				3.2
Ho	0.19			0.09				0.60
Er	0.4			0.2				1.6
Tm	<0.1			<0.1				0.2
Yb	0.40			0.30	1.27	0.70	1.80	1.40
Lu	0.05			<0.05	0.19	0.10	0.29	0.22

Note: Major, trace, and rare-earth element analyses were performed at XRAL Laboratories, Don Mills, Ont., Canada. Major elements and Rb, Sr, Zr, Y, except for samples 95PRP1, 96HP2, 96HP3, 96BH2, and 96BH3, which were analyzed by neutron activation. Detection limits are 0.01% for major elements limits for REE analyzed by neutron activation are 3 ppm for Nd, 1 ppm for Ce, 0.1 ppm for La and Tb, 0.05 for Eu and Yb, and 0.01 for Sm and Lu.

[a]A, amphibolite; G, granite; GD, granodiorite; GrtG, garnet granite; QD, quartz diorite; QFG, quartzofeldspathic gneiss; QM, quartz monzonite.

geographic variation in initial ε_{Nd}: the values for southern gneisses are generally more negative than those for the central gneisses (Fig. 12A). Initial $^{87}Sr/^{86}Sr$ isotopic data likewise range from depleted mantle values to more radiogenic compositions ($^{87}Sr/^{86}Sr$ = 0.7003 to 0.7112, plus 0.7320; Table 4). There is a general, though imperfect, correlation between initial ε_{Nd} and $^{87}Sr/^{86}Sr$ compositions (Fig. 12A) consistent with derivation of the samples from multiple sources that include ones with depleted mantle compositions and ones with more evolved isotopic compositions typical of older continental crust. The distinctive unradiogenic Nd and radiogenic Sr isotopic compositions of sample 97BNE3 deserve comment. This sample is the most siliceous of the gneiss samples, but no field, petrographic, or geochemical features

set it apart from the others. We note, however, that middle Archean rocks with similarly unradiogenic Nd isotopic compositions are present in the northern Granite Mountains, less than 100 km south of this sample locality (Fruchey 2002; Grace et al. 2006).

The younger granitoids of the Bighorn Mountains, including samples from the 2.85 Ga Bighorn batholith and a 2.89 Ga tonalitic pluton in the central Bighorn Mountains, are characterized by less variable initial ε_{Nd} and $^{87}Sr/^{86}Sr$ compositions (Table 4; Fig. 12B). Their initial Nd isotopic compositions lie within the field of the older Bighorn gneisses and are +1.5 for the 2.89 Ga tonalite and between +0.3 and –2.5 for the Bighorn batholith. The initial ε_{Nd} compositions of gneisses from the western Owl Creek Moun-

96HP2 QFG	96HP3 A	96LH1 QFG	96LH3 QFG	96PRP1 QFG	97BNE1 QFG	97BNE2 QFG	97BNE3 QFG	97BNE5 QFG	97BNE6 QFG	97BNE7 QFG
66.6	49.4	66.3	69.7	64.1	61.1	71.2	75.3	74.0	60.5	74.3
0.48	0.87	0.74	0.33	0.59	0.79	0.31	0.18	0.19	0.26	0.08
16.1	13.9	16.1	14.3	16.1	16.4	14.6	13.2	14.0	20.0	13.9
3.12	11.34	4.28	2.48	4.34	5.80	2.57	1.59	1.76	3.33	1.46
0.05	0.18	0.05	0.02	0.05	0.09	0.03	0.01	0.02	0.04	0.01
1.54	7.93	1.68	0.75	1.48	2.45	0.64	0.36	0.54	1.32	0.20
4.23	11.00	4.38	2.89	4.68	5.91	2.99	1.48	1.93	8.95	2.46
5.24	1.60	3.99	3.83	4.27	4.08	4.13	3.17	3.54	3.41	3.89
0.07	0.16	1.42	3.02	1.53	1.50	1.98	4.23	3.61	0.46	2.55
0.11	0.06	0.19	0.11	0.15	0.22	0.10	0.06	0.11	0.06	0.02
0.25	0.50	0.30	0.55	0.40	0.45	0.35	0.45	0.25	0.45	0.35
97.80	96.94	99.43	97.98	97.68	98.78	98.90	100.03	99.95	98.78	99.22
0.98	0.61	1.00	0.96	0.94	0.86	1.02	1.06	1.06	0.89	1.02
0.67	0.59	0.72	0.77	0.75	0.70	0.80	0.82	0.76	0.72	0.88
1.08	–9.24	1.03	3.96	1.12	–0.33	3.12	5.92	5.22	–5.08	3.98
	6	72	70	57	34	62	145	104	9	41
191	108	359	216	434	268	235	96	159	164	306
155	51	173	204	158	175	181	118	85	100	154
18	23	14	5	8	19	9	7	2	11	
5	10	7	4	3	8	6	7	7	2	4
199	68	567	970	490	790	784	942	786	120	2040
15.9	2.7	49.3	65.0	13.8	25.3	39.1				61.3
29.0	7.0	91.1	118.0	32.0	50.9	63.4				95.3
13.0	5.0	35.7	42.0	12.8	24.0	23.0				29.8
2.04	1.86	6.00	6.10	2.60	4.80	3.30				3.80
0.81	0.79	1.67	1.32	0.87	1.42	0.93				1.19
		5.0	4.3	2.2	4.8	2.9				2.6
0.2	0.4	0.7	0.5	0.3	0.7	0.4				0.3
		3.2	1.6	1.6	3.9	1.8				0.8
		0.60	0.27	0.30	0.76	0.35				0.13
		1.6	0.6	0.8	2.1	1.0				0.4
		0.2	<0.1	0.1	0.3	0.2				<0.1
0.70	1.80	1.40	0.70	0.80	2.00	1.00				0.40
0.10	0.29	0.22	0.12	0.12	0.33	0.18				0.08

Nb, and Ba were analyzed by X-ray fluorescence (XRF). Rare-earth elements were determined by inductively coupled plasma – mass spectrometry (ICP–MS) and 2 ppm for Rb, Sr, Zr, Y, Nb, and Ba. Detection limits for REE analyzed by ICP–MS are 0.1 ppm, except 0.05 ppm for Eu, Ho, and Lu. Detection A/CNK, alumina saturation index; LOI, loss on ignition; MALI, modified alkali-lime index, $Na_2O + K_2O-CaO$; $Fe^* = FeO^t/(FeO^t + MgO)$.

tains and Washakie block are similar to those of the Bighorn batholith, with the exception of a hornblende tonalite gneiss from the Owl Creek Mountains that has an initial ε_{Nd} value of 3.7, close to the composition of contemporary depleted mantle (Fig. 12B). Except for this one sample, all the others require the incorporation of material from a source with less radiogenic Nd isotopic compositions than that of depleted mantle. The 2.95 Ga Bighorn gneiss terrain is one such possible source that satisfies the Nd–Sr isotopic requirements (Fig. 12B).

The Pb isotopic data from rocks of the BBMZ are consistent with the involvement of radiogenic upper crust in their formation (Fig. 13). Initial Pb isotopic compositions of western Owl Creek Mountain gneisses were determined from the least radiogenic ratios obtained from step-dissolved feldspar (Table 5). These data, along with the feldspar Pb-isotope ratio of Native Lake gneiss (Frost et al. 1998) and eastern Beartooth Mountains (Wooden and Mueller 1988), define a cluster that lies above the model upper continental crust of Zartman and Doe (1981) and may be interpreted as requiring the incorporation of older crustal components. To generate the measured initial Pb isotopic compositions of these rocks at 2.95 Ga, the Pb reservoir would have to separate from the Zartman and Doe model mantle at ca. 3.60 Ga and have a µ value ($^{238}U/^{204}Pb$) of between 14 and 17. Later separation, for example at 3.20 Ga, would require a correspondingly higher µ of 25–35 (Fig. 13) to generate the $^{207}Pb/^{204}Pb$ values but may not explain some low $^{206}Pb/^{204}Pb$ values of the feld-

Table 2 (*concluded*).

Sample No.:	Granitic rocks from Bighorn batholith, northern Bighorn Mountains							
	96BH1	96BH2	96BH3	96BH4	96BH5	96BH6	96BH7	96BH8
Description:[a]	G	QM	G	GD	G	G	QD	GD
SiO_2 (wt.%)	72.0	72.9	72.3	69.0	72.4	70.6	50.7	70.3
TiO_2	0.30	0.24	0.24	0.55	0.19	0.17	1.35	0.34
Al_2O_3	13.6	13.5	14.3	14.5	14.7	15.2	13.6	14.7
FeO^t	1.83	1.66	1.94	3.98	1.44	1.18	11.25	2.54
MnO	0.02	0.01	0.01	0.05	0.01	0.01	0.19	0.02
MgO	0.42	0.29	0.44	1.49	0.48	0.63	6.28	0.87
CaO	1.73	1.64	2.29	3.17	2.38	2.94	9.96	2.81
Na_2O	3.76	3.11	3.55	3.85	3.93	4.06	3.21	4.02
K_2O	4.04	5.54	3.69	2.36	3.51	2.97	0.68	2.59
P_2O_5	0.06	0.08	0.09	0.19	0.06	0.11	0.11	0.12
LOI	0.90	0.75	0.65	0.55	0.40	0.25	0.20	0.30
Total	98.66	99.72	99.50	99.69	99.50	98.12	97.53	98.61
A/CNK	0.99	0.96	1.02	0.99	1.01	1.00	0.56	1.01
Fe^*	0.81	0.85	0.82	0.73	0.75	0.65	0.64	0.74
MALI	6.07	7.01	4.95	3.04	5.06	4.09	−6.07	3.80
Rb (ppm)	131	148	60	84	64	52	6	62
Sr	184	339	303	205	348	404	155	393
Zr	329	313	249	253	95	189	103	136
Y		32	22	46		4	26	
Nb	17	15	7	13	3	3	2	3
Ba	612	1040	1500	702	1000	1180	88	875
La	37.2	103.0	20.4	55.5	32.1			49.8
Ce	64.4	171.0	35.0	105.0	56.1			92.9
Nd	22.0	53.0	12.0	45.0	19.2			26.4
Sm	3.10	7.24	1.88	8.50	2.60			3.20
Eu	1.02	1.25	0.91	1.68	0.80			0.98
Gd	2.5			8.1	1.8			2.0
Tb	0.3	0.6	0.2	1.3	0.2			0.2
Dy	1.2			6.5	0.6			0.8
Ho	0.22			1.23	0.10			0.13
Er	0.6			3.6	0.3			0.3
Tm	<0.1			0.5	<0.1			<0.1
Yb	0.60	1.27	0.60	3.20	0.30			0.30
Lu	0.10	0.18	0.09	0.45	0.06			<0.05

spars and calculated whole rock initials. Contamination of model mantle by continental crust older than 3.60 Ga to generate elevated $^{207}Pb/^{204}Pb$ values does not explain the samples with the most radiogenic initial Nd isotopic compositions and elevated $^{207}Pb/^{204}Pb$.

Other models for the Pb isotopic evolution of the Archean mantle (i.e., Luais and Hawkesworth 2002) do not require such early separation of continental crust from mantle. Based on Pb isotopic values of two samples with initial Nd isotopic compositions closest to those of depleted mantle (samples 95LH3 and 98OC4), the mantle reservoir for the Wyoming Province may have had evolved Pb isotopic compositions at 2.95–2.84 Ga and μ values of 8.50–8.65 (Tables 5, 6; Fig. 13). Continental crust separated from this model mantle at 3.30 Ga with μ values of only 10–16 would have appropriate isotopic values for the range of initial Pb isotopic values for the

2.95–2.85 Ga gneisses of the BBMZ (Fig. 13). Mixtures of a high-μ mantle reservoir and slightly more evolved 3.30 Ga continental crust could explain the variation observed in the Pb data from the BBMZ, without requiring significantly older crust. Evidence for 3.30–3.10 Ga crust in the Wyoming Province includes the 3.30 Ga Sacawee block of south-cental Wyoming (Kruckenberg et al. 2001; Fruchey 2002; Grace et al. 2006), U–Pb ages of gneisses in the Beartooth Mountains (Mueller et al. 1996), and inherited zircon cores in 2.95 Ga Bighorn gneisses (Frost and Fanning 2006). Evidence for ca. 3.60 Ga and older crust includes a 3.50 Ga trondhjemite near the northwestern boundary of the BBMZ (Mueller et al. 1996) and as a few inherited and detrital zircons detected in younger gneisses (Aleinikoff et al. 1989; Mueller et al. 1992, 1998; Kruckenberg et al. 2001).

Present-day Pb isotopic compositions of whole rocks from

96BH9 GD	97BH2 G	97BH3 GD	97BH5 GD	97BH6 GD	97BNE4 GrtG
70.1	75.1	70.5	71.9	64.8	75.8
0.21	0.26	0.73	0.32	0.7	0.02
15.6	12.9	13.2	13.9	16.4	13.0
1.59	1.32	3.66	2.41	4.18	0.53
0.01	0.01	0.03	0.04	0.05	0.05
0.59	0.31	0.92	0.79	1.22	0.06
3.07	1.05	2.53	1.76	4.03	0.93
4.87	3.1	3.74	3.82	4.6	2.98
1.61	5.04	2.83	3.33	2.29	5.26
0.05	0.04	0.14	0.11	0.23	0.04
0.50	0.25	0.90	0.50	0.45	0.05
98.21	99.38	99.18	98.88	98.95	98.72
1.02	1.03	0.96	1.06	0.94	1.06
0.73	0.81	0.80	0.75	0.77	0.90
3.41	7.09	4.04	5.39	2.86	7.31
41	70	36	165	27	137
553	134	258	164	514	70
119	137	304	143	306	67
	12	27	17	15	15
3	5	8	10	6	
612	653	954	493	1730	745
19.8					5.9
33.4					11.5
11.4					4.2
1.80					0.80
0.65					0.50
1.3					1.0
0.2					0.3
0.5					2.3
0.08					0.65
0.2					2.4
<0.1					0.4
0.20					3.30
<0.05					0.52

the Bighorn Mountains and Washakie block plot in an array with a slope of a 2.85–0 Ga isochron that projects back to the fields defined by feldspar separates from the Beartooth, Owl Creek, and Wind River ranges (Fig. 13) (see also Mogk et al. 1992; Fig. 4). Therefore, late Archean magmatic rocks from throughout the BBMZ are characterized by elevated initial $^{207}Pb/^{204}Pb$ ratios, well above the upper crustal model values of Zartman and Doe (1981). The samples from the southern Bighorn gneiss terrain are offset to slightly more radiogenic $^{207}Pb/^{204}Pb$ ratios than the samples from the central and northern Bighorn Mountains, a feature that is consistent with their slightly less radiogenic Nd isotopic compositions (Fig. 12A).

It is noteworthy that, whereas the Bighorn samples have Rb, Sr, Sm, and Nd concentrations and Rb/Sr and Sm/Nd ratios typical of felsic continental crust, their U concentrations

are relatively low: the $^{238}U/^{204}Pb$ ratios (μ) for the Bighorn samples average 4.1, much lower than that of typical continental crust (Table 6) (cf. Stacey and Kramers 1975). Pb concentrations are <20 ppm, and therefore the low U/Pb is not the result of high Pb concentrations, nor is it the result of recent U loss, since many of the calculated initial whole rock Pb isotopic compositions plot within the field defined by feldspar Pb from the BBMZ (Table 6; Fig. 13). Calculated Th/U ratios are high, in part because of the low U concentrations of these rocks. Calculated $^{232}Th/^{204}Pb$ ratios are quite variable, ranging from 6.2 to 138.0 for these rocks, and half the samples have $^{232}Th/^{204}Pb$ higher than that of average crust ($^{232}Th/^{204}Pb$ = 38.6). Wooden and Mueller (1988) observed similar low U/Pb and variable Th/U ratios in the rocks of the eastern Beartooth Mountains; it appears that low U/Pb and variable Th/U ratios are a characteristic of rocks across the BBMZ.

Discussion

Extent of 3.00–2.80 Ga quartzofeldspathic basement in the Wyoming Province

In addition to the uplifts studied here, the eastern Beartooth Mountains expose a large area of ca. 2.80–2.83 Ga magmatic rocks (P.A. Mueller, personal communication, 2006). Three compositional groups have been recognized, including the Long Lake granite (LLG in Fig. 7) that exhibits gradational contacts with the Long Lake granodiorite (LLGd in Fig. 7) and a variety of biotite–hornblende quartz diorites and amphibolites referred to as "andesitic amphibolite" (Mueller et al. 1988; Wooden et al. 1988). The granitic to granodioritic rocks are compositionally similar to the samples from the Bighorn, Owl Creek, and Wind River uplifts reported here: they span the magnesian–ferroan and metaluminous–peraluminous boundaries and include both calcic and calc-alkalic compositions. Most of the eastern Beartooth samples are medium to high K and are similar in major element compositions to the Bighorn batholith granites and granodiorites. Interestingly, there is a group of sodic granitoids identified by Mueller et al. (1988) as the high-Na subset of the Long Lake granite, which is compositionally indistinguishable from the tonalitic gneisses of the central Bighorn Mountains and a number of similar rocks in the western Owl Creek Mountains and Washakie block (fields in Figs. 7A–7C).

The REE patterns of the Long Lake granite and granodiorite mirror the variations exhibited in the Bighorn batholith. The Long Lake granodiorite has moderately LREE enriched patterns with negative europium anomalies, patterns similar to those of samples 96BH2 and 96BH4. The Long Lake granite has REE patterns with extreme HREE depletion and no europium anomaly, features that typify Archean TTG suites (Martin 1994). The overall variation in REE patterns is indistinguishable from 3.00–2.80 Ga samples elsewhere in the Wyoming Province (cf. Figs. 10A–10E).

Like their counterparts elsewhere in the central Wyoming Province, eastern Beartooth rocks have Sr, Nd, and Pb isotopic compositions that differ from those of model depleted mantle sources: the initial Pb isotopic compositions are very radiogenic (Fig. 13), the initial Sr isotopic compositions are slightly

Table 3. Geochemical data for quartzofeldspathic gneisses of the western Owl Creek Mountains and Washakie block, Wind River Range.

	Western Owl Creek Mountains									Washakie block, Wind River Range		
Sample No.:	98OC2	98OC4	98OC6	98OC7	98OC8	98OC19	98OC20	98OC21	98OC22	94Bob1	95Bob12	95Bob10
Description:[a]	GDG	HTG	BTG	GG	GDG	GDG	HTG	GDG	GG	NG	BG	BG
SiO_2 (wt.%)	72.9	64.0	70.4	74.8	68.5	69.5	68.0	73.7	74.6	64.8	73.5	68.8
TiO_2	0.16	0.66	0.17	0.03	0.62	0.30	0.43	0.17	0.01	0.55	0.09	0.35
Al_2O3	15.2	16.0	15.8	13.5	14.7	15.9	15.0	14.8	14.2	16.0	15.4	14.8
FeO^t	1.31	5.14	1.52	0.51	4.14	1.73	3.84	0.86	0.23	4.93	0.64	3.54
MnO	0.01	0.07	0.01	0.01	0.04	0.02	0.06	0.01	0.01	0.08	0.02	0.07
MgO	0.42	2.09	0.50	0.07	1.27	0.58	1.46	0.32	0.06	2.17	0.15	1.61
CaO	2.22	5.22	3.15	0.97	3.11	2.79	3.93	2.37	1.16	5.06	2.09	3.41
Na_2O	5.96	4.37	5.37	3.32	3.78	5.91	4.34	5.35	4.44	3.82	5.29	3.28
K_2O	0.98	1.38	1.14	5.66	2.53	1.31	1.18	1.52	4.52	1.14	2.49	2.85
P_2O_5	0.02	0.22	0.04	0.01	0.14	0.07	0.14	0.04	0.01	0.11	0.02	0.10
LOI	0.20	0.35	0.20	0.01	0.40	0.20	0.25	0.20	0.05	0.95	0.20	0.70
Total	99.38	99.50	98.30	98.89	99.23	98.31	98.63	99.34	99.29	99.62	99.89	99.51
A/CNK	1.02	0.91	1.01	1.01	1.03	0.99	0.99	1.01	0.99	0.96	1.01	1.01
Fe^*	0.76	0.71	0.75	0.88	0.77	0.75	0.72	0.73	0.79	0.72	0.83	0.71
MALI	4.72	0.53	3.36	8.01	3.20	4.43	1.59	4.50	7.80	–0.10	5.69	2.72
Rb (ppm)	30	45	18	87	71	56	30	9	76	30	29	86
Sr	322	376	439	195	205	503	277	380	218	323	671	225
Zr	140	227	145	46	399	199	171	152	40	110	75	113
Y	3	25	1	2	14	2	4	1	2	6	3	24
Nb	11	73	10	20	10	10	9	4	6	5	4	6
Ba	101	611	522	1350	1230	384	421	749	1330	595	1250	1200
La	25.0	22.6	10.5		78.6			21.3		17.8		
Ce	49.2	57.9	17.6		147.0			31.1		31.1		
Nd	19.9	31.9	5.1		46.1			9.2		12.7		
Sm	3.3	7.0	0.7		6.5			1.1		2.8		
Eu	0.25	1.39	0.45		0.88			0.51		0.97		
Gd	2.4	5.7	0.5		5.9			0.9		2.2		
Tb	0.2	0.9	0.1		0.5			0.1		0.4		
Dy	0.7	4.8	0.1		2.7			0.2		2.1		
Ho	0.1	0.9	0.1		0.5			0.1		0.4		
Er	0.2	2.8	0.1		1.3			0.1		1.1		
Tm	0.1	0.4	0.1		0.1			0.1		0.2		
Yb	0.1	2.0	0.1		1.0			0.1		1.0		
Lu	0.10	0.33	0.10		0.10			0.10		0.20		

Note: Major, trace, and rare-earth element analyses were performed at XRAL Laboratories, Don Mills, Ont., Canada. Major elements and Rb, Sr, Zr, Y, Nb, and Ba were analyzed by XRF. Rare-earth elements were determined by ICP–MS. Detection limits are 0.01% for major elements and 2 ppm for Rb, Sr, Zr, Y, Nb, and Ba. Detection limits for REE are 0.1 ppm except 0.05 ppm for Eu, Ho, and Lu. LOI, loss on ignition; A/CNK, alumina saturation index; $Fe^* = FeO^t/(FeO^t + MgO)$; MALI, modified alkali-lime index, $Na_2O + K_2O–CaO$.
[a]BG, banded gneiss; BTG, biotite tonalite gneiss; GDG, granodiorite gneiss; GG, granite gneiss; HTG, hornblende tonalite gneiss; NG, native gneiss.
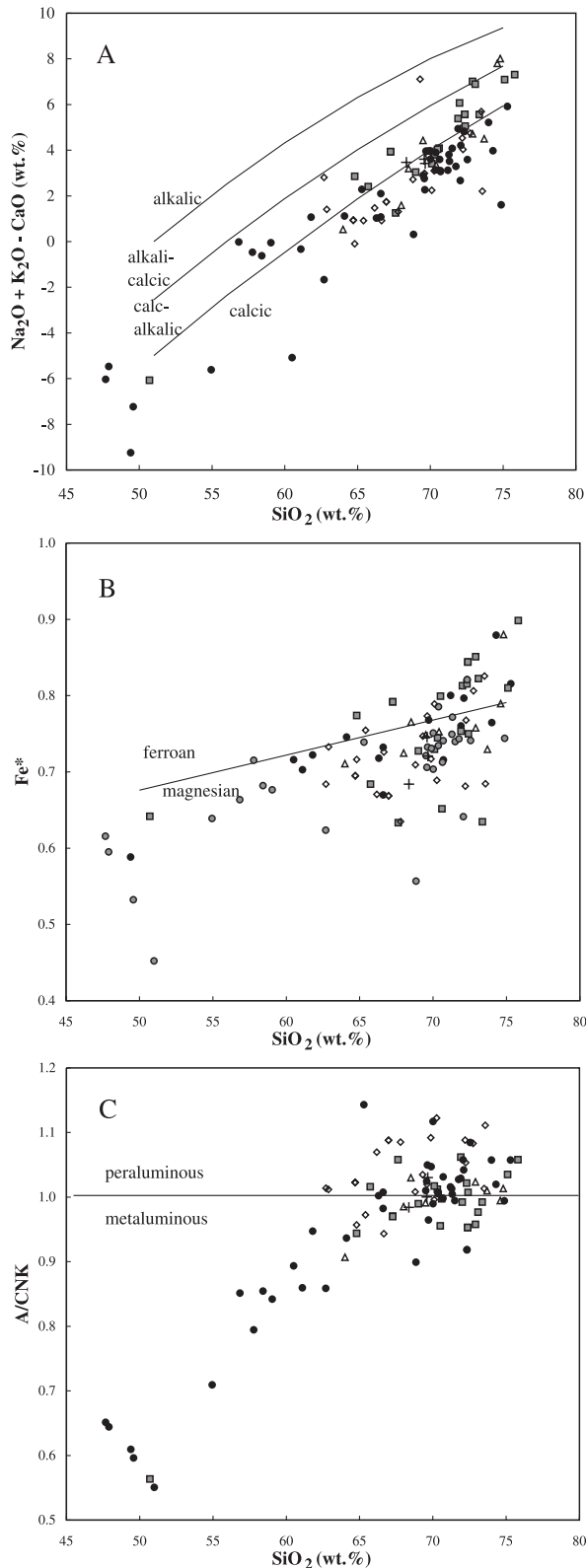
Fig. 6. (A) Plot of $(Na_2O + K_2O)–CaO$ as a function of SiO_2 content for Archean rocks of the Bighorn batholith (shaded squares), Bighorn gneiss terrain (solid circles), western Owl Creek Mountains (open triangles), and Washakie block of the Wind River Range (open diamonds). Also shown are average TTG (+ symbols) from Martin et al. (2005). Most samples are calcic according to the classification of Frost et al. (2001), but Bighorn batholith samples are typically calc-alkalic. A few alkali-calcic rocks occur in all three uplifts. (B) $Fe^*[FeO^t/(FeO^t + MgO)]$ versus SiO_2 content for the same sample set, indicating most samples are magnesian, but that some of the more siliceous rocks are ferroan. (C) Aluminum saturation index as a function of SiO_2 content, showing that most samples are slightly peraluminous, in particular almost all the samples from the Washakie block. Data from Tables 2 and 3, Barker et al. (1979), Frost et al. (1998), Heimlich (1971), and Osterwald (1955).

and Mueller et al. (1996) and extend it to include portions of the Owl Creek and Wind River uplifts. It seems extremely likely that all the ca. 3.00–2.80 Ga quartzofeldspathic rocks of the Wyoming Province share a common petrogenesis.

Origin of the TTG suite

The TTG-affinity gneisses of the Wyoming Province place important constraints on models for the formation of Archean tonalite–trondhjemite–granodiorite suites. Although most models of TTG genesis propose that TTG can be derived solely by partial melting of hydrated mafic lower crust, the rocks studied here indicate that their petrogenesis is more complex. In particular, we note that their isotopic compositions require involvement of preexisting isotopically evolved crustal sources, and that the presence of both TTG- and calc-alkalic-affinity rocks of the same age is not adequately explained by existing models of TTG formation.

Models for TTG genesis invoke partial melting of a tholeiitic garnet amphibolite leaving a residue that includes hornblende and garnet to produce trondhjemitic liquids with HREE depletion (Barker and Arth 1976; Martin 1987). Experimental studies confirm that 10%–40% partial melting of hydrous metabasalt at pressures above the garnet-in boundary produces the requisite major element compositions, as well as other key trace element characteristics (Rapp and Watson 1995; Rapp et al. 2003). Supporting this model are initial Sr and Nd isotopic compositions of TTG suites that are close to mantle values (Martin 1994). Initial $^{87}Sr/^{86}Sr$ ratios tend to be low, typically between 0.701 and 0.703 (O'Nions and Pankhurst 1978; Arth et al. 1980; Martin et al. 1983), and initial ε_{Nd} values in many suites are positive (i.e., Martin et al. 1983; Henry et al. 1998). On the other hand, some TTG suites include samples with negative initial ε_{Nd} values (i.e., Berger and Rollinson 1997; Whalen et al. 2002; this study). These variations may reflect heterogeneity of the mafic source or the incorporation of old sialic crust, possibilities we address later in the paper.

Although the paucity of mafic and intermediate rocks in Archean gray gneiss terrains presents a serious limitation to an origin for the TTG suite solely by fractional crystallization of a hydrous basaltic magma, it does appear that late-stage fractional crystallization may account for some of the dispersion in geochemical compositions. In studies of TTG suites in

radiogenic, and the initial ε_{Nd} compositions are slightly negative. These characteristics, which are common throughout the BBMZ, indicate the involvement of a ≥3.60 Ga crustal reservoir or a high-μ mantle reservoir and 3.30 Ga crust. On the basis of these similarities, we can confirm the identification of a BBMZ as originally proposed by Mogk et al. (1992)

Fig. 7. (A) Na_2O, (B) K_2O, and (C) Na_2O/K_2O as a function of SiO_2 for Archean rocks of the Bighorn Mountains, western Owl Creek Mountains, and northeastern Wind River Range. Symbols as in Fig. 6. Shown for comparison are fields for data from the eastern Beartooth Mountains (Mueller et al. 1988), indicating that the 2.83–2.80 Ga Long Lake granodiorite (LLGd) and Long Lake granite (LLG) are similar in composition to rocks elsewhere in the Beartooth–Bighorn magmatic zone.

Fig. 8. Al_2O_3 plotted as a function of SiO_2 content for Archean rocks from the Bighorn Mountains, western Owl Creek Mountains, and Washakie block of the northeastern Wind River Range. Most samples have greater than 15% Al_2O_3 at 70% SiO_2; these samples are high-Al_2O_3 trondhjemites by the classification of Barker (1979). Symbols as in Fig. 6.
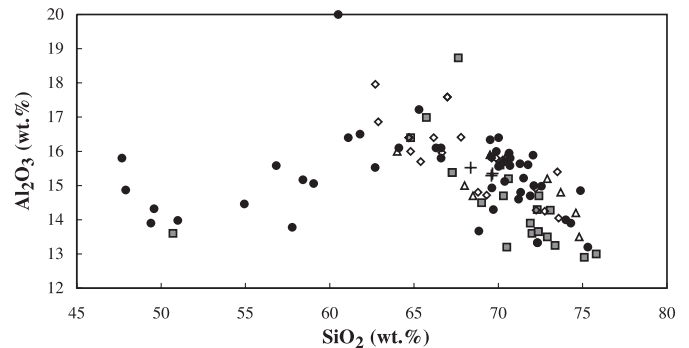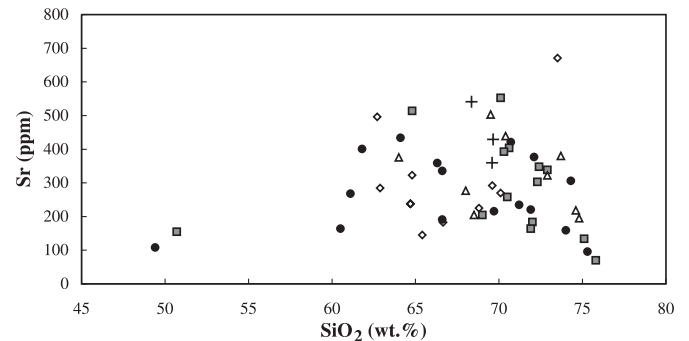

Fig. 9. Sr contents versus SiO_2 content for Archean rocks from the Bighorn Mountains, western Owl Creek Mountains, and Washakie block of the northeastern Wind River Range. Symbols as in Fig. 6.

southwestern and eastern Finland, respectively, Arth et al. (1978) and Martin (1987) used geochemical modeling to illustrate that fractionation of plagioclase and hornblende produced a greater HREE depletion, the development of concavity in the HREE pattern, and a positive Eu anomaly,

features that characterized the most felsic members of the suites. Geochemical modeling is complicated by the fact that, due to their cumulate nature, the rock compositions may not be identical to liquid compositions. Moreover, modeling of REE contents is difficult due to the presence of small amounts of accessory minerals that fractionate REEs (Bea 1996). It nevertheless appears that fractional crystallization is important in producing the limited diversity in Archean TTG suites.

Martin and Moyen (2002) suggested that Archean TTG suites underwent a change in composition with time. Their examination of the most primitive members of TTG occurrences led them to propose that Mg# and Ni and Cr contents of TTG increase between 4.00 and 2.50 Ga, which they explained by increased interactions between TTG melts and

mantle peridotite. An increase in Sr, and to a lesser extent $Na_2O + CaO$, was interpreted to indicate a declining role for plagioclase in the residua. Martin and Moyen related these changes to increasing depth of slab melting and greater interaction with increasing thicknesses of mantle wedge with time. Smithies et al. (2003) likewise suggested that TTG magmas did not interact with a mantle wedge prior to ~3.10 Ga but attributed this to a uniquely Archean tectonic process involving partial melting of thick mafic crust, built by an underplating process they referred to as "Archean flat-subduction".

Wyoming TTG suites appear to be typical of Archean TTG worldwide, with the possible exception of the more peraluminous compositions of Washakie block gneisses. One important feature of Wyoming Province TTG that is not well-explained by current models for TTG formation is their occurrence together with high-K gneisses and granitoids. In places where age relations are well established, such as in the Bighorn Mountains, potassic granodiorites and granites intrude a mixture of GG-affinity gneisses and TTG-affinity gneisses. In other places the TTG and GG rocks appear to be essentially synchronous, such as in the western Owl Creek Mountains and the eastern Beartooth Mountains. A second significant characteristic of Wyoming TTG is that their Sr, Nd, and Pb isotopic compositions mostly differ from those of contemporary depleted mantle sources. Both initial Nd and Sr isotopic ratios extend from a few samples with depleted mantle compositions to ratios typical of a more evolved reservoir such as older silicic crust. $^{207}Pb/^{204}Pb$ ratios are particularly radiogenic, higher than both the model crust of Stacey and Kramers (1975) and the upper crust of Zartman and Doe (1981). All three isotopic systems require that the protolith of these TTGs include a component with a substantial crustal prehistory.

Geochemical and isotopic modeling is complicated because the Wyoming TTGs do not represent a single magmatic series but instead were intruded over a period of time from multiple magma batches. Nevertheless, several features of these rocks help to place limits on the possible petrogenetic processes. First, the interaction of mafic and older silicic components must have taken place deep in the crust to stabilize garnet in the residue. The Pb and Nd isotopic compositions of the rocks indicate that the silicic contaminant was old, high-μ crust with a model age of at least 3.20 Ga and probably older (Figs. 12, 13). The crustal contaminant appears to have been slightly different in the southern Bighorn Mountains, where the TTG samples have more radiogenic $^{207}Pb/^{204}Pb$ and more negative initial ε_{Nd} than elsewhere. This area is close to the Granite Mountains, where the oldest rocks in the central Wyoming Province are found (Fruchey 2002; Grace et al. 2006). Because the gneisses in the eastern Beartooth Mountains have relatively homogeneous isotopic compositions, Wooden and Mueller (1988) suggested that early and middle Archean sediments may have been subducted into the mantle, creating an enriched mafic source from which TTG rocks could be extracted. The presence of some TTG samples with depleted mantle Nd and Sr isotopic compositions complicates this hypothesis, however. We suggest a simpler explanation in which partial melting of basaltic rocks at the base of the crust also partially melted overlying silicic material

with geographically variable isotopic compositions. A model involving assimilation of felsic crust during ascent is supported by the presence of inherited, >3.00 Ga old zircon in TTG in the Bighorn Mountains, both low-U zircon typical of lower crustal sources and higher U zircon typical of felsic rocks from the middle and upper crust (Frost and Fanning 2006).

The data from the TTG in the Wyoming Province are not the only data that challenge the assumption that TTGs are generated solely by partial melting of basaltic sources. Whalen et al. (2002) argue based on elevated $\delta^{18}O$ and variable initial ε_{Nd} values that crustal recycling was an important process in the formation of TTG in the Wabigoon subprovince of the Superior Province. Berger and Rollinson (1997) present data strikingly similar to those of the present study from anhydrous TTG-affinity rocks of the Northern Marginal Zone of the Limpopo Belt in southern Zimbabwe. They argue that their 2.70 Ga suite of rocks, which also have elevated initial $^{207}Pb/^{204}Pb$ ratios and include negative initial ε_{Nd} values, were formed by interaction of an old, high-μ, low-Sm/Nd crustal component and a younger, low-μ, high-Sm/Nd mantle-derived component. They point out that assimilation and fractional crystallization (AFC) processes can buffer isotopic compositions through rapidly rising elemental compositions as a result of fractional crystallization, and that therefore it is not necessary to invoke an enriched mantle source to explain the existence of old, high-μ crustal provinces.

Origin of the potassic, GG suite

The potassic granitoid rocks of the BBMZ are composed of high-K, calc-alkalic granodiorites and granites (Figs. 5, 6A, 7B) that have lower Na_2O contents than the TTG suite but equally variable REE patterns, ranging from LREE-enriched patterns with negative Eu anomalies to patterns with extreme HREE depletion and absent to positive Eu anomalies (Fig. 10). Their initial ε_{Nd} values define a narrower spread of values than the TTG suite, and they lie within the range defined by the TTG suite (Fig. 12B). Their Pb isotopic compositions are indistinguishable from those of the TTG samples (Fig. 13). These isotopic characteristics are compatible with the interpretation that the potassic granitoids and the TTG rocks are derived from similar sources and include the possibility that the potassic granitoids are formed by partially melting TTG-composition crust. Experimental results reported by Skjerlie et al. (1993) establish that the potassic granitoid compositions can be produced by partial melting of tonalitic gneiss, although partial melting of tonalitic gneiss at 10 kbar (1 kbar = 100 MPa) produces only 5%–7% of weakly peraluminous granitic melt at a temperature of 950 °C. If the tonalites were interlayered with pelitic rocks, the melt fraction would increase significantly, but the melt composition would be more alkalic than the rocks of the BBMZ (Skjerlie et al. 1993). The HREE depletion observed in many of the potassic granitoids is compatible with experimental results showing that garnet is present in the restite (Skjerlie et al. 1993). We conclude that partial melting of TTG gneisses in the middle to lower continental crust can produce potassium-rich, calc-alkalic rocks with the observed geochemical and isotopic compositions, although the volume of calc-alkalic rocks made
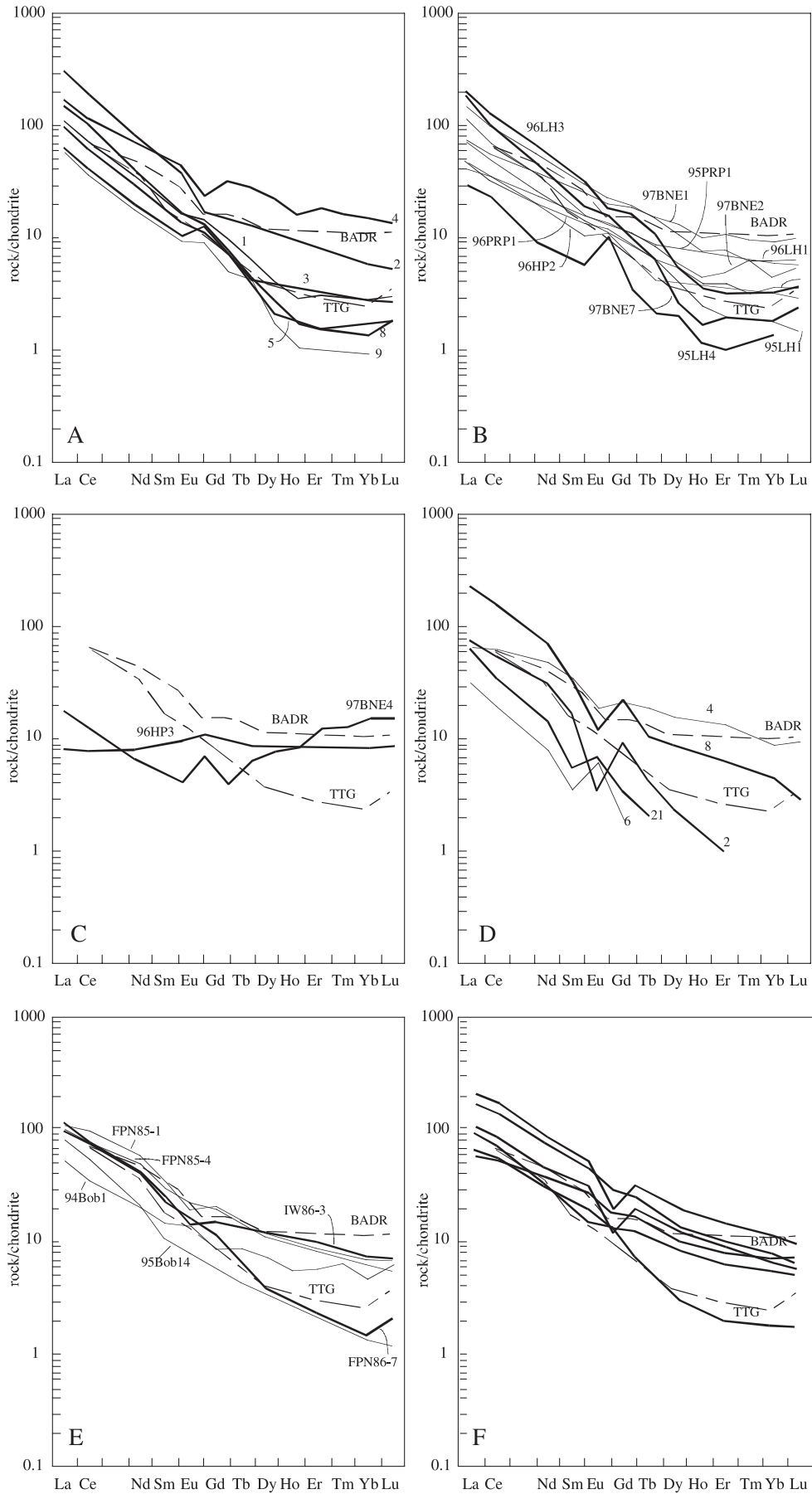
Fig. 10. Chondrite-normalized rare-earth element abundances for Archean rocks from the Beartooth–Bighorn magmatic zone. Thick lines are calc-alkalic samples, and thin lines are calcic, TTG-affinity samples. (A) Bighorn batholith. (B) Bighorn gneisses. (C) Bighorn Mountains (quartz diorite sample 96HP3; garnet granite sample 97BNE4). (D) Western Owl Creek Mountains. (E) Washakie block. (F) Samples from the 2.63 Ga Louis Lake batholith in the central Wind River Range plotted to illustrate that this continental-arc calc-alkalic batholith includes samples with the same HREE depletion that characterizes many of the older TTG-affinity gneisses. Data from Tables 2 and 3, Frost et al. (1998), and Frost et al. (2000). Also plotted using broken lines are average TTG (Martin 1994) and calc-alkalic basalt–andesite–dacite–rhyolite (BADR) (Smithies 2000). Chondrite normalizing values are from Wakita et al. (1971).

Fig. 11. Plot of SiO_2 versus La/Lu, showing that low-silica samples generally have lower $(La/Lu)_N$, corresponding to less steep REE patterns, but that higher SiO_2 samples exhibit a large range in $(La/Lu)_N$. Symbols as in Fig. 6.
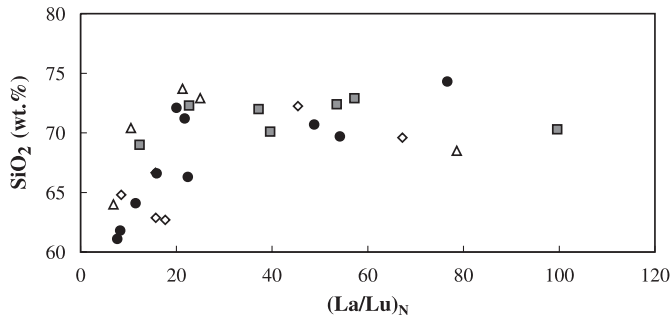
by this process will be small compared with the volume of TTG rocks.

Younger, voluminous, late Archean calc-alkalic batholiths composed of granodiorites and granites occur as elongate belts along the southern and western margins of the Wyoming Province. Principal among these are the 2.67 Ga Bridger batholith, which is exposed in the central and northern Wind River Range, and the 2.63 Ga Louis Lake batholith and 2.62 Ga Granite Mountains batholith, which are located in the central and southern Wind River Range and the Granite Mountains, respectively (Stuckless and Miesch 1981; Frost et al. 1998). These batholiths are calc-alkalic to alkali-calcic, metaluminous to weakly peraluminous, and magnesian to ferroan, and their compositional ranges are comparable to those of modern subduction-related batholiths. These batholiths have been interpreted as the product of continental-arc magmatism akin to modern subduction-related continental margin batholiths (Frost et al. 1998). Like modern arc-related magmas (and unlike the older Wyoming Province calc-alkalic rocks), their isotopic compositions require that they are composed of both depleted mantle and crustal sources (Fig. 12B). Their REE patterns, however, include some similar to those of the steep, HREE-depleted compositions that are thought to typify Archean TTG (Fig. 10F). Clearly, REE patterns alone do not identify Archean TTG.

In summary, the potassic granodiorites and granites of the BBMZ are distinct from TTG-affinity rocks and from the younger, subduction-related calc-alkalic batholiths. We interpret them as having formed by partial melting of preexisting TTG crust, thereby inheriting the isotopic characteristics of that protolith. The process appears to have occurred repeatedly in the late Archean: this study has described potassic granitoid rocks occurring together with tonalitic rocks within the 2.95 Ga central and southern Bighorn gneiss terrain, in the 2.86–2.84 Ga Bighorn batholith, in the 2.84–2.82 Ga western Owl Creek Mountains, and in the 2.83–2.80 Ga

Long Lake granite of the Beartooth Mountains. Farther south in the Granite Mountains, the ca. 3.30 Ga calc-alkalic Sacawee orthogneiss is exposed adjacent to the approximately coeval tonalitic UC Ranch orthogneiss, indicating that both calc-alkalic- and TTG-affinity rocks are present even in the oldest parts of the province (Fruchey 2002; S.C. Kruckenberg, unpublished data). It seems probable that the same events that partially melted mafic rocks to form TTG may also have provided the heat to melt older TTG crust and form modest volumes of potassic granitoids. This petrogenesis is distinct from that for continental-arc granitoids, which include juvenile components from the downgoing slab and (or) mantle wedge as well as from overlying continental crust. The role of juvenile, mantle-derived magma sources is readily identified in the latest Archean continental-arc batholiths of the southwestern Wyoming Province, whose Nd-isotope compositions extend from depleted mantle values into the range of compositions for older Wyoming Province crust (Fig. 12B).

A model for the TTG–GG transition in Archean cratons

Archean terrains are commonly described as being composed of two quite distinct groups of granitoids: an older, sodic, TTG-affinity group, and a late Archean potassium-rich group (e.g., Taylor and McLennan 1985). The change, which some authors place at around 2.75 Ga (Taylor and McLennan 1985) and others at 2.50 Ga (Martin 1994), is said to mark a mineralogical and geochemical shift in granitoid composition that is related to a change in magma sources, particularly the availability of metasomatized mantle wedge sources only from late Archean to the present (Martin 1994). In the Wyoming Province, the transition from TTG to more potassic granitoids is not a sharp one, but rather these two rock suites occur together for a substantial period of the Archean, spanning at least 500 million years. This long transition is not unique to the Wyoming Province. A similar pattern is observed in the eastern Pilbara craton, which is composed of felsic igneous rocks of at least seven distinct ages, from 3.50 to 2.80 Ga (Smithies et al. 2003). The oldest of these are TTG compositions with very fractionated REE patterns and depleted HREE contents (Bickle et al. 1993), whereas the younger Archean plutonic rocks include some with the chemical and isotopic characteristics of the older suites, but they also include calc-alkalic granodiorite and granite with less fractionated REE patterns and negative europium anomalies. Nd isotopic data were interpreted to suggest that the younger granites may be formed by partial melting of the older TTG crust (Bickle et al. 1989), an origin analogous to the origin proposed here for the older potassic granitoid rocks of the Wyoming Province. Bickle et al. (1993) also observed that the distinction between TTG and GG

Table 4. Nd and Sr isotopic data for Archean rocks from the Bighorn and western Owl Creek Mountains and Washakie block of the Wind River Range.

Sample No.	Rb (ppm)	Sr (ppm)	$\frac{^{87}Rb}{^{86}Sr}$	$\frac{^{87}Sr}{^{86}Sr}$	Initial $\frac{^{87}Sr}{^{86}Sr}$	Sm (ppm)	Nd (ppm)	$\frac{^{147}Sm}{^{144}Nd}$	$\frac{^{143}Nd}{^{144}Nd}$	Initial $\frac{^{143}Nd}{^{144}Nd}$	Initial ε_{Nd}	T(CR) (Ga)
Quartzofeldspathic gneiss of the central Bighorn Mountains (initials calculated at 2885 Ma)												
95LH1	40.69	431.39	0.2731	0.71438	0.70296	8.58	55.99	0.0926	0.510734	0.508970	1.5	3.0
Quartzofeldspathic gneisses of the central and southern Bighorn Mountains (initials calculated at 2950 Ma)												
95LH2	57.55	323.05	0.5164	0.72582	0.70373	6.48	43.36	0.0904	0.510647	0.508886	1.6	3.1
95LH3	90.46	203.24	1.2944	0.75832	0.70295	4.46	26.95	0.1001	0.510946	0.508997	3.7	2.9
95LH4	36.22	350.43	0.2994	0.71582	0.70302	0.90	5.06	0.1070	0.510762	0.508678	−2.5	3.4
95PRP1	66.98	398.14	0.4875	0.72168	0.70082	2.87	14.46	0.1198	0.511195	0.508861	1.1	3.2
96HP2	0.99	165.12	0.0174	0.70551	0.70477	2.34	13.25	0.1066	0.510977	0.508899	1.8	3.1
96HP3	2.77	103.07	0.0778	0.70366	0.70033	2.20	6.74	0.1974	0.512751	0.508905	2.0	
96LH1	63.78	345.67	0.5349	0.72586	0.70297	4.64	27.54	0.1019	0.510855	0.508871	1.3	3.1
96LH3	66.30	218.92	0.8792	0.73997	0.70236	5.10	35.67	0.0865	0.510590	0.508905	1.9	3.1
96PRP1	47.01	450.12	0.3025	0.71709	0.70415	2.01	10.24	0.1185	0.511061	0.508753	−1.0	3.3
97BNE1	28.77	273.12	0.3051	0.71694	0.70389	3.78	18.61	0.1227	0.511146	0.508756	−1.0	3.3
97BNE2	43.14	191.27	0.6542	0.73099	0.70300	2.67	17.25	0.0936	0.510751	0.508928	2.4	3.0
97BNE3	115.10	92.53	3.6633	0.88829	0.73157	1.86	8.93	0.1262	0.510759	0.508301	−9.9	4.1
97BNE5	95.25	157.61	1.7623	0.78657	0.71118	1.53	8.99	0.1030	0.510628	0.508622	−3.6	3.5
97BNE6	6.58	170.61	0.1117	0.70667	0.70189	6.28	35.08	0.1082	0.510882	0.508774	−0.6	3.3
97BNE7	34.00	292.61	0.3366	0.71708	0.70268	3.04	24.32	0.0756	0.510304	0.508832	0.5	3.1
Granitic rocks of the Bighorn batholith (initials calculated at 2845 Ma)												
96BH1	91.52	167.18	1.5952	0.77897	0.71320	2.26	15.95	0.0858	0.510497	0.508885	−1.2	3.1
96BH2	105.92	291.04	1.0577	0.75155	0.70795	6.05	45.90	0.0797	0.510388	0.508892	−1.0	3.1
86BH3	40.96	265.58	0.4470	0.72348	0.70505	1.83	12.56	0.0880	0.510573	0.508921	−0.4	3.1
96BH4	71.40	190.05	1.0919	0.75190	0.70688	6.87	36.81	0.1128	0.511052	0.508933	−0.2	3.2
96BH5	42.93	321.70	0.3868	0.72372	0.70777	2.02	15.60	0.0784	0.510289	0.508817	−2.5	3.2
96BH6	43.27	384.90	0.3256	0.71703	0.70361	2.54	18.67	0.0823	0.510413	0.508867	−1.5	3.2
96BH7	3.30	155.99	0.0612	0.70463	0.70211	3.16	11.60	0.1647	0.512052	0.508958	0.3	
96BH8	58.49	330.11	0.5134	0.72092	0.69975	3.31	27.01	0.0741	0.510237	0.508845	−1.9	3.2
96BH9	29.45	525.86	0.1621	0.70991	0.70323	1.47	9.44	0.0943	0.510684	0.508914	−0.6	3.1
97BH2	58.93	134.37	1.2754	0.75886	0.70628	10.23	63.70	0.0971	0.510720	0.508898	−0.9	3.2
97BH3	28.35	262.24	0.3131	0.71688	0.70397	19.70	144.90	0.0822	0.510467	0.508924	−0.4	3.1
97BH5	133.16	157.97	2.4669	0.82309	0.72139	4.33	25.94	0.1009	0.510755	0.508860	−1.7	3.2
97BH6	20.45	492.09	0.1202	0.70728	0.70232	9.22	68.65	0.0812	0.510437	0.508913	−0.6	3.1
Garnet granite of the southern Bighorn Mountains (initials calculated at 2630 Ma)												
97BNE4	119.48	67.48	5.2362	0.93128	0.73203	0.65	3.21	0.1216	0.511095	0.508986	−4.7	3.4
Quartzofeldspathic gneiss of the western Owl Creek Mountains (initials calculated at 2820 Ma)												
98OC2	30.11	368.07	0.2369	0.71555	0.70586	3.25	17.81	0.1105	0.510913	0.508857	−2.4	3.3
98OC4	43.04	356.88	0.3493	0.71828	0.70401	6.54	32.23	0.1226	0.511446	0.509163	3.7	2.8
98OC6	28.21	539.20	0.1514	0.70840	0.70221	1.58	11.34	0.0840	0.510371	0.508808	−3.3	3.2

Table 4 (*concluded*).

Sample No.	Rb (ppm)	Sr (ppm)	$\frac{^{87}Rb}{^{86}Sr}$	$\frac{^{87}Sr}{^{86}Sr}$	Initial $\frac{^{87}Sr}{^{86}Sr}$	Sm (ppm)	Nd (ppm)	$\frac{^{147}Sm}{^{144}Nd}$	$\frac{^{143}Nd}{^{144}Nd}$	Initial $\frac{^{143}Nd}{^{144}Nd}$	Initial ε_{Nd}	T(CR) (Ga)
98OC8	83.79	219.33	1.1097	0.74576	0.70042	6.96	49.00	0.0859	0.510470	0.508872	−2.1	3.2
98OC19	52.93	447.20	0.3428	0.71647	0.70246	0.49	3.54	0.0831	0.510571	0.509025	0.9	3.0
98OC20	29.50	251.74	0.3394	0.71559	0.70173	1.85	12.94	0.0864	0.510573	0.508964	−0.3	3.1
98OC21	13.10	334.68	0.1132	0.70736	0.70273	1.54	12.61	0.0740	0.510411	0.509034	1.1	3.0
98OC22	71.94	202.93	1.0296	0.74487	0.70280	0.29	2.14	0.0828	0.510556	0.509015	0.7	3.0
Quartzofeldspathic gneiss of the Washakie terrane, northeast Wind River Mountains (initials calculated at 2840 Ma)												
95Bob5[a]	12.48	176.20	0.2050	0.71138	0.70300	1.92	14.38	0.0806	0.510541	0.509029	1.0	3.0
95Bob14[a]	48.09	381.20	0.3654	0.71815	0.70322	2.21	14.42	0.0925	0.510712	0.508978	0.0	3.1
FPN85-1[a]	72.01	284.80	0.7331	0.73115	0.70120	8.60	48.58	0.1070	0.510902	0.508896	−1.6	3.2
FPN85-4[a]	91.92	496.40	0.5364	0.72329	0.70137	7.11	36.09	0.1191	0.511140	0.508907	−1.4	3.2
FPN86-7[a]	61.82	169.90	1.0536	0.75152	0.70847	4.70	28.54	0.0995	0.510749	0.508884	−1.9	3.2
FPN86-10[a]	11.77	152.60	0.2233	0.71062	0.70150	10.90	43.28	0.1523	0.511806	0.508952	−0.5	3.3
IW86-3[a]	64.10	182.50	1.0197	0.74577	0.70411	5.67	31.07	0.1103	0.510847	0.508779	−3.9	3.4
94Bob1	23.35	274.32	0.2464	0.71385	0.70379	1.97	10.41	0.1145	0.511118	0.508972	−0.1	3.1
95Bob12	13.82	588.99	0.0679	0.70728	0.70450	0.39	3.04	0.0768	0.510429	0.508988	0.2	3.0
95Bob3	27.40	221.79	0.3580	0.72082	0.70619	1.54	10.78	0.0865	0.510536	0.508914	−1.3	3.1
FPN94-7	57.28	122.98	1.3543	0.75615	0.70082	8.13	32.82	0.1498	0.511817	0.509010	0.6	3.2
95Bob10	81.27	200.26	1.1795	0.75178	0.70358	2.37	9.28	0.1542	0.511819	0.508928	−1.0	

Note: Approximately 80–100 mg of sample were dissolved in HF–HNO$_3$. After conversion to chlorides, one third of the sample was spiked with ^{87}Rb, ^{84}Sr, ^{149}Sm, and ^{146}Nd. Rb, Sr, and REE were separated by conventional cation-exchange procedures. Sm and Nd were further separated in di-ethyl-hexyl orthophosphoric acid columns. All isotopic measurements were made on a VG Sector multicollector mass spectrometer at the University of Wyoming. An average ^{87}Sr/^{86}Sr isotopic ratio of 0.710251 ± 20 (2σ) was measured for National Bureau of Standards NBS 987 Sr, and an average ^{143}Nd/^{144}Nd ratio of 0.511846 ± 11 (2σ) was measured for the LaJolla Nd standard. Uncertainties are ±0.00002 in Sr isotopic ratio measurements and ±0.00001 (2σ) in Nd isotopic ratio measurements. Blanks are <50 pg for Rb, Sr, Nd, and Sr, and no blank correction was made. Uncertainties in Rb, Sr, Nd, and Sm concentrations are ±2% of the measured value; uncertainties on initial ε$_{Nd}$ = ±0.5 epsilon units. Initial Sr and Nd isotopic ratios and initial ε$_{Nd}$ values are calculated for 170 Ma. Nd model ages (T(CR)) are calculated based on the depleted mantle model of Goldstein et al. (1984) for samples with ^{147}Sm/^{144}Nd < 0.15.

[a]Frost et al. (1998).

Table 5. Feldspar Pb isotopic results from the western Owl Creek Mountains and Washakie block.

Sample No.	Phase	$\dfrac{^{206}Pb}{^{204}Pb}$	$\dfrac{^{207}Pb}{^{204}Pb}$	$\dfrac{^{208}Pb}{^{204}Pb}$
Washakie block, Wind River Range				
FPN85-4	K-feldspar	14.186	15.094	33.876
Western Owl Creek Mountains				
98OC2	K-feldspar	13.823	14.974	33.818
98OC4	Plagioclase	13.884	15.009	33.517
Model mantle[a]		13.447	14.921	
98OC6	Plagioclase	13.874	15.041	33.864
98OC8	K-feldspar	13.971	15.094	34.314

Note: Isotopic compositions of feldspar are from analyses of the least radiogenic dissolution step dissolved in 5% HF after Ludwig and Silver (1977). Analytical details and uncertainties are described in Table 6.

[a]Wyoming Province model mantle (μ = 8.65) reservoir values at 2.84 Ga calculated after Luais and Hawkesworth (2002) using feldspar Pb isotopic values from sample 98OC4 and single stage growth from Canyon Diablo meteorite values (98OC4 has near depleted mantle ϵ_{Nd} value at 2.84 Ga).

series rocks is not clear-cut, for example, that there is no consistent correlation between less and more fractionated REE types and the degree of K/Na enrichment or depletion.

The tectonic setting for the production of Archean TTG and potassic GG suites is problematic. Clearly, Phanerozoic TTG suites are formed in modern plate tectonic environments. Tonalitic rocks occur in the Early Cretaceous Separation Point batholith of New Zealand (Muir et al. 1995); the Cretaceous Peninsular Ranges Batholith (Gromet and Silver 1987); the Cordillera Blanca batholith, Peru (Petford and Atherton 1996); and plutons in the Klamath Mountains and Blue Mountains (Barnes et al. 1996; Johnson et al. 1997). In all these locations, production of tonalites and trondhjemites with fractionated REE patterns is attributed to partial melting of mafic crust at depths at which garnet is a stable residual phase.

These examples of Phanerozoic TTG therefore suggest that the processes forming Archean TTG could be similar to modern plate tectonics. Some of the features that we observe in the Phanerozoic examples appear to be absent in Archean terrains, however. For example, the pre-2.70 Ga rocks of the Wyoming Province do not preserve evidence of elongate magmatic arc batholiths with compositional zoning parallel to the elongation direction that is characteristic of the younger intrusions (Muir et al. 1995; Gromet and Silver 1987). Although it is possible that limited exposure of Archean rocks in the Wyoming Province may prevent us from identifying such spatial patterns, in the Pilbara craton similar batholiths containing both potassic, calc-alkalic and TTG-type granitoids are well exposed. These granitoid batholiths exhibit striking domiform outcrop patterns unlike those of modern batholithic belts (Bickle et al. 1993). We concur with other workers that alternative mechanisms to modern-style plate tectonics may have produced the Archean TTG and associated potassic granitoids (e.g., Smithies 2000; Martin et al. 2005).

Accordingly, we propose a model for the formation of Archean granitoids that invokes distinctly Archean tectonics until the latest Archean. The first stages of this model are adopted from Smithies et al. (2003), who proposed that

Fig. 12. Nd and Sr isotopic data for the late Archean rocks of the Wyoming Province. (A) Initial Nd and Sr isotopic compositions of the ca. 2.95 Ga gneisses of the central and southern Bighorn Mountains, showing that all samples are displaced from model depleted mantle compositions towards the more evolved compositions of older continental crust. Samples from the southern Bighorn Mountains (solid circles) have on average more negative initial ϵ_{Nd} and more radiogenic initial $^{87}Sr/^{86}Sr$ than samples from the central Bighorn Mountains, perhaps reflecting the presence of older or more isotopically evolved continental crust in the south. (B) Initial ϵ_{Nd} plotted as a function of crystallization age for granitoids of the Wyoming Province. The 2.95 Ga gneisses from the Bighorn Mountains are heterogeneous with respect to initial ϵ_{Nd}, and most of the younger rocks of the Beartooth–Bighorn magmatic zone (BBMZ) lie within the evolution path of these older rocks. The samples from the Bighorn gneiss terrain and western Owl Creek sample with depleted mantle compositions are sodic, tonalite gneisses that apparently interacted less with isotopically evolved components than did other samples. Samples from the Bridger and Louis Lake calc-alkalic batholiths in the Wind River Range have initial ϵ_{Nd} that range between depleted mantle compositions and the evolution path of BBMZ rocks and thus require the incorporation of juvenile components. Data from Table 4, Frost et al. (1998), and Wooden and Mueller (1988). cont. arcs, continental arcs.
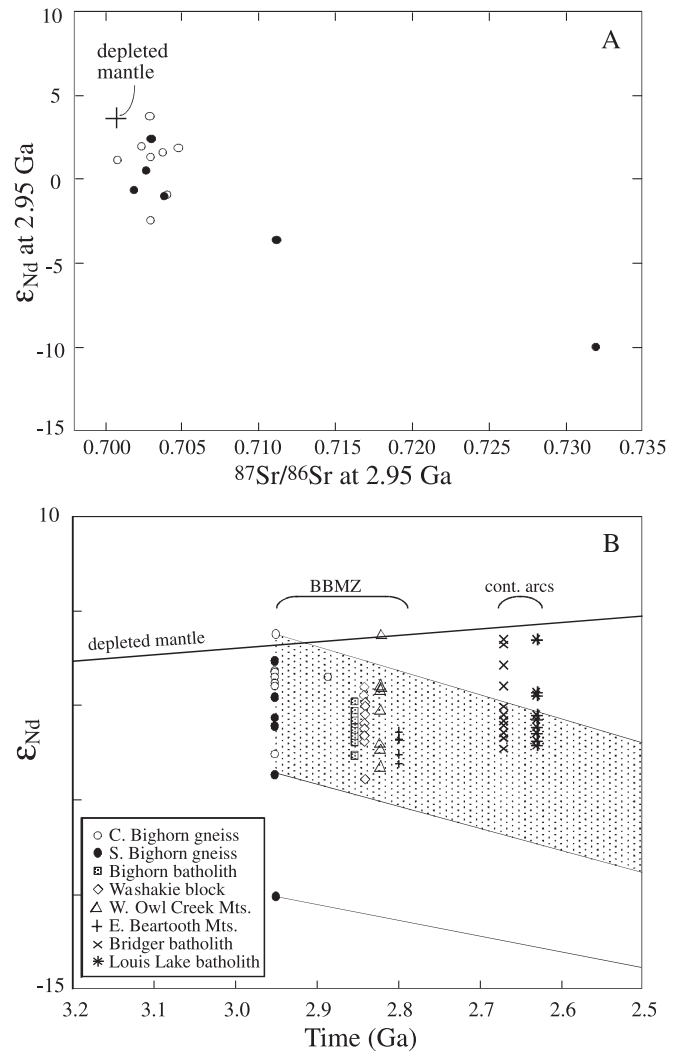
Table 6. Whole rock Pb isotopic results from 2.80–2.90 Ga rocks of the Wyoming Province.

Sample No.	$\dfrac{^{206}Pb}{^{204}Pb}$	$\dfrac{^{207}Pb}{^{204}Pb}$	$\dfrac{^{208}Pb}{^{204}Pb}$	U (ppm)	Pb (ppm)	$\dfrac{^{238}U}{^{204}Pb}$	Initial $\dfrac{^{206}Pb}{^{204}Pb}$	Initial $\dfrac{^{207}Pb}{^{204}Pb}$	Th/U	$\dfrac{^{232}Th}{^{204}Pb}$
Quartzofeldspathic gneiss of the central Bighorn Mountains (initials calculated at 2.89 Ga)										
95LH1	15.239	15.175	37.173	0.21	9.2	1.4	14.465	15.014	8.7	13.8
Quartzofeldspathic gneisses of the central and southern Bighorn Mountains (initials calculated at 2.95 Ga)										
95LH2	16.133	15.366	50.373	0.62	10.4	4.3	13.649	14.830	26.0	128.5
95LH3	16.185	15.377	41.289	1.16	17.0	4.4	13.657	14.832	11.6	58.5
Model mantle[a]						8.5	13.145	14.721		
95LH4	14.544	15.066	35.177	0.22	14.0	0.9	14.029	14.955	7.1	7.3
95PRP1	19.687	16.032	37.381	0.57	7.0	5.2	16.671	15.381	2.3	14.0
96LH1	20.956	16.302	43.527	1.15	9.8	8.2	16.171	15.269	5.1	48.3
96LH3	16.464	15.414	43.176	0.81	10.0	5.3	13.373	14.746	13.0	80.0
96PRP1	18.220	15.775	37.173	0.50	6.6	4.7	15.474	15.182	2.9	15.9
97BNE1	15.799	15.393	36.873	0.33	7.8	2.6	14.313	15.072	5.8	17.2
97BNE2	18.087	15.797	40.256	0.57	9.7	3.8	15.868	15.318	5.6	24.9
97BNE3	18.603	16.033	42.433	0.70	16.4	2.9	16.941	15.674	6.7	22.2
97BNE5	15.641	15.397	35.962	0.43	21.4	1.2	14.952	15.248	4.5	6.2
97BNE6	17.663	15.781	44.585	0.35	7.8	3.1	15.891	15.398	10.3	36.5
97BNE7	15.718	15.374	45.763	0.49	13.2	2.5	14.277	15.063	22.8	65.4
Granitic rocks of the Bighorn batholith (initials calculated at 2.85 Ga)										
96BH1	17.080	15.556	46.027	0.84	9.0	6.4	13.524	14.834	13.7	101.1
96BH2	26.125	17.440	61.030	1.69	14.9	10.4	20.345	16.267	8.1	97.7
96BH3	15.853	15.323	36.443	0.55	9.2	3.5	13.880	14.923	4.9	20.0
96BH4	19.321	16.008	42.365	1.48	11.0	9.2	14.226	14.974	5.7	60.9
96BH5	16.346	15.406	41.916	0.45	11.5	2.5	14.945	15.121	11.7	34.1
96BH6	15.049	15.184	41.745		10.8				23.0	
96BH7	17.030	15.577	35.498	0.46	4.7	5.8	13.810	14.923	2.1	13.9
96BH8	14.647	15.046	41.678	0.23	6.3	2.3	13.383	14.790	33.0	86.8
96BH9	14.409	14.998	36.174	0.12	8.6	0.8	13.952	14.905	14.1	13.5
97BH2	14.573	15.028	42.414	0.20	7.6	1.7	13.648	14.840	39.3	75.6
97BH3	15.953	15.287	52.595	0.31	6.0	3.8	13.855	14.861	31.6	138.0
97BH5	21.711	16.553	46.541	2.25	17.3	9.7	16.339	15.463	5.9	66.5
97BH6	14.513	15.020	41.073	0.12	6.4	1.2	13.848	14.885	35.9	49.6
Garnet granite of the southern Bighorn Mountains (initials calculated at 2.63 Ga)										
97BNE4	15.849	15.487	34.889	0.57	12.9	2.5	14.566	15.260	2.1	6.3

Note: Lead and uranium were purified in the feldspar and whole rock samples using HCl–HBr chemistry, modified from Tilton (1973). Pb and U samples were loaded onto single rhenium filaments with silica gel and graphite, respectively, for isotopic analysis on a VG Sector 54 mass spectrometer. Mass discrimination factors of 0.127 ± 0.06% for Pb and 0 ± 0.06% for U were determined by multiple analyses of NBS SRM 981 and U-500, respectively. PBDAT (Ludwig 1988) was used to reduce raw mass spectrometer data, correct for blanks, and calculate uncertainties, which are 0.12%, 0.18%, and 0.24% on $^{206}Pb/^{204}Pb$, $^{207}Pb/^{204}Pb$, and $^{208}Pb/^{204}Pb$, respectively. Th/U ratios were calculated based on growth from feldspar compositions from crystallization age to the present. $^{208}Pb/^{235}U$ tracer used to measure U and Pb concentrations and $^{238}U/^{204}Pb$ was calibrated against MIT2 gravimetric standard and yielded a $^{206}Pb/^{238}U$ date of 419.26 ± 0.47 Ma for zircon standard R33 in good agreement with Royal Ontario Museum (ROM) date (Black et al. 2004).

[a]Wyoming Province model mantle reservoir values at 2.95 Ga calculated after Luais and Hawkesworth (2002) using whole rock Pb isotopic values from 95LH3 and single-stage growth from Canyon Diablo meteorite values (95LH3 has near depleted mantle ε_{Nd} value at 2.95 Ga).

"Archean flat-slab subduction" led to underplating of thick, hot, and hydrated oceanic crust (Fig. 14A). Alternatively, a thick basaltic crust may have formed above mantle upwellings (Bédard 2006). Evidence for a mafic lower crust in the Wyoming Province is provided by the Deep Probe geophysical transect (Snelson et al. 1998; Gorman et al. 2002), which imaged a 15–20 km thick, high-velocity, dense lower crust beneath the BBMZ. The age of this mafic layer is unknown. It appears to extend beneath the entire BBMZ, although it may be somewhat thinner south of the Owl Creek Mountains (Snelson et al. 1998). This high-velocity lower crustal layer could represent the Archean mafic lower crustal source of the type envisioned by Smithies et al. (2003) and Bédard (2006).

In the second stage of the model, the lower part of the thickened mafic crust melts, producing TTG melt and an eclogitic residue. As eclogite is delaminated, either as inverted diapirs or by tectonic delamination, fertile mantle wells up and provides heat for additional TTG production and a source of basalt for supracrustal successions (Smithies et al. 2003; Bédard 2006) (Fig. 14B). This heating event may also induce partial melting within the TTG-composition crust, producing

Fig. 13. Pb isotopic compositions of whole rock samples and step-dissolved feldspar from Archean intrusive rocks of the Bighorn, Wind River, and western Owl Creek Mountains, central Wyoming Province. The model upper crust and mantle curves of Zartman and Doe (1981) (ZD) are plotted for reference. Calculated Pb isotopic initial compositions of whole rock samples plot within the dark shaded field. The compositions of feldspar from the western Owl Creek Mountains plot in the field labeled O. Also plotted are the fields for initial Pb isotopic compositions from the eastern Beartooth Mountains from Wooden and Mueller (1988) and the Wind River Range from Frost et al. (1998), labeled E and W, respectively. A high-μ model mantle reservoir for the Wyoming Province is also plotted after Luais and Hawkesworth (2002). Secondary isochrons run from Zartman and Doe (ZD) (1981) model mantle values indicate that the initial high $^{207}Pb/^{204}Pb$ of samples requires involvement of Pb from a continental source extracted from the mantle 3.6 billion years ago. Mixtures of high-μ mantle and 3.30 Ga continental crust may provide a better fit to the Pb data.
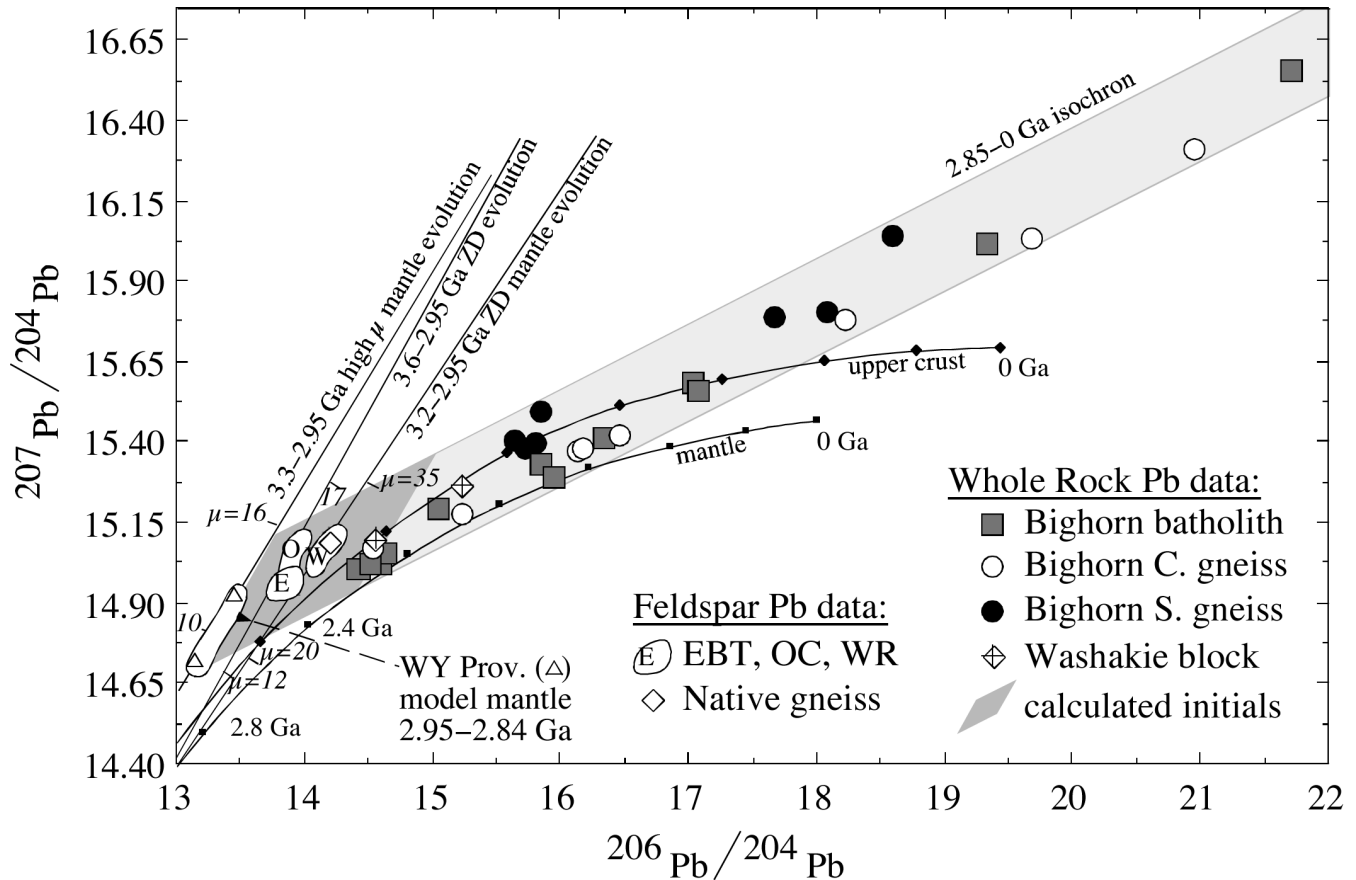
small volumes of potassic granitoids and their eruptive equivalents. To account for multiple ages of TTG and potassic GG rocks in Archean provinces, we suggest that this process must have been repeated multiple times to account for the repeated co-occurrence of TTG and potassic granitoids in the Wyoming Province and Pilbara craton.

In the final stage of the model, corresponding to late Archean time, elongate, calc-alkalic continental-arc batholiths form from depleted mantle and older crustal sources, suggesting that modern-style subduction zone processes operated (Fig. 14C). In the Wyoming Province, this process began around 2.70 Ga with the formation of the Bridger batholith, followed at 2.62–2.63 Ga by the Louis Lake and Granite Mountains batholiths (Fig. 12B). We note that similar magmatic arc rocks dominate the late Archean history of the Superior Province (Henry et al. 1998, 2000). Subduction-related calc-alkalic magmatism may have been delayed in other Archean cratons such as the Slave, where late Archean granitoids "bloom" across the entire province instead of forming linear belts (Davis and Bleeker 1999), or the Yilgarn, where

the compositions of late Archean granitoids cannot all be explained by subduction-related tectonic processes (Champion and Sheraton 1997). However prolonged the transition, continental-arc magmatism is the dominant process in Phanerozoic time, when potassic, calc-alkalic rocks are widespread and TTG rocks are formed in lesser volumes only under special conditions.

Acknowledgments

Fig. 14. Cartoon showing possible model for the origin of Archean TTG and calc-alkalic suites in the Wyoming Province. (A) Thickened mafic crust partially melts to form TTG-composition magmas (2.80–3.00 Ga). Assimilation of older middle and upper crust imparts its isotopically evolved signature to the TTG magmas. (B) Continued partial melting produces more TTG magma and eclogitic restite (2.80–3.00 Ga). The restite delaminates, and fertile magma wells up, providing a source of basalt for supracrustal belts and heating the crust, inducing partial melting of TTG to make small volumes of calc-alkalic magma. (C) By 2.67 Ga, more voluminous subduction-related calc-alkalic magmatism takes place along the margins of the Wyoming Province. Model adapted from Smithies et al. (2003) and Bédard (2006).
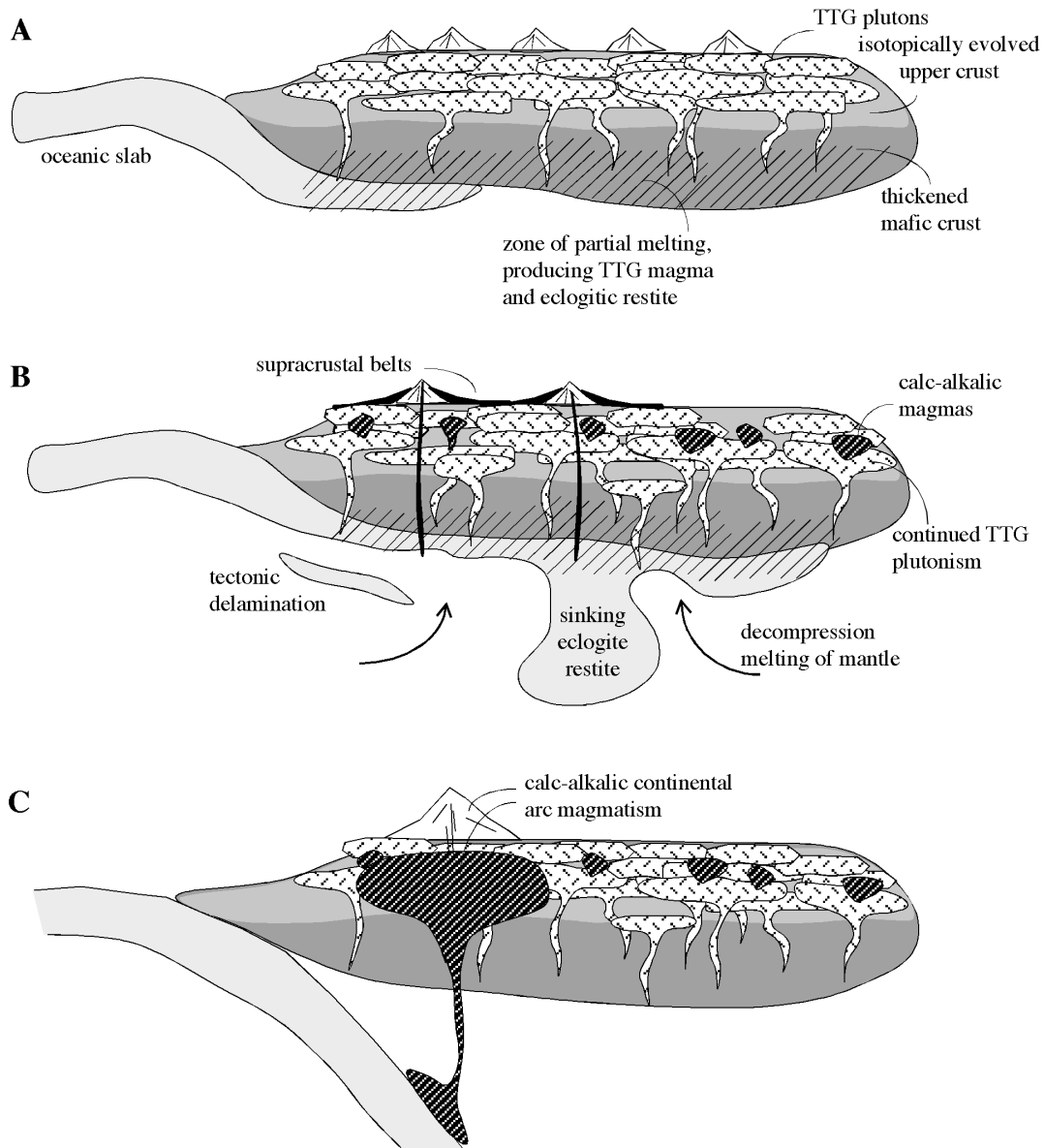
References

Aleinikoff, J.N., Williams, I.S., Compston, W., Stuckless, J.S., and Worl, R.G. 1989. Evidence for an Early Archean component in the Middle to Late Archean gneisses of the Wind River Range, west-central Wyoming: conventional and ion microprobe U–Pb data. Contributions to Mineralogy and Petrology, **101**: 198–206.

Armbrustmacher, T.J. 1972. Mafic dikes of the Clear Creek drainage, southern Bighorn Mountains. University of Wyoming Contributions to Geology, **11**: 31–39.

Arth, J.G., Barker, F., Peterman, Z.E., and Friedman, I. 1978. Geochemistry of the gabbro–diorite–tonalite–trondhjemite suite of southwest Finland and its implications for the origin of tonalitic and trondhjemitic magmas. Journal of Petrology, **19**: 289–316.

Arth, J.G., Barker, F., and Stern, T.W. 1980. Geochronology of Archean gneisses in the Lake Helen area, southwestern Big Horn Mountains, Wyoming. Precambrian Research, **11**: 1–22.

Barker, F. 1979. Trondhjemite: definition, environment and hypotheses of origin. *In* Trondhjemites, dacites, and related rocks. *Edited by* F. Barker. Elsevier, Amsterdam, The Netherlands, pp. 1–12.

Barker, F. 1982. Geologic map of the Lake Helen quadrangle, Big Horn and Johnson counties, Wyoming. US Geological Survey, Map GQ-1563, 1 sheet. Scale 1 : 24 000.

Barker, F., and Arth, J.G. 1976. Generation of trondhjemitic–tonalitic

liquids and Archean bimodal trondhjemite–basalt suites. Geology, **4**: 596–600.

Barker, F., Arth, J.G., and Millard, H.T., Jr. 1979. Archean trondhjemites of the southwestern Big Horn Mountains, Wyoming: a preliminary report. *In* Trondhjemites, dacites, and related rocks. *Edited by* F. Barker. Elsevier, Amsterdam, The Netherlands, pp. 401–414.

Barnes, C.G., Petersen, S.W., Kistler, R.W., Murray, R., and Kays, M.A. 1996. Source and tectonic implications of tonalite–trondhjemite magmatism in the Klamath Mountains. Contributions to Mineralogy and Petrology, **123**: 40–60.

Bea, F. 1996. Residence of REE, Y, Th and U in granites and crustal protoliths: implications for the chemistry of crustal melts. Journal of Petrology, **37**: 521–552.

Bédard, J.H. 2006. A catalytic delamination-driven model for coupled genesis of Archean crust and sub-continental lithospheric mantle. Geochimica et Cosmochimica Acta, **70**: 1188–1214.

Berger, M., and Rollinson, H. 1997. Isotopic and geochemical evidence for crust–mantle interaction during late Archean crustal growth. Geochimica et Cosmoschimica Acta, **61**: 4809–4829.

Bickle, M.J., Bettenay, L.F., Chapman, H.J., Groves, D.E., McNaughton, N.J., Campbell, I.H., and de Laeter, J.R. 1989. The age and origin of younger granitic plutons of the Shaw Batholith in the Archaean Pilbara Block, Western Australia. Contributions to Mineralogy and Petrology, **101**: 361–376.

Bickle, M.J., Bettenay, L.F., Chapman, H.J., Groves, D.E., McNaughton, N.J., Campbell, I.H., and de Laeter, J.R. 1993. Origin of the 3500–3300 Ma calc-alkaline rocks in the Pilbara Archaean: isotopic and geochemical constraints from the Shaw Batholith. Precambrian Research, **60**: 117–149.

Black, L.P., Kamo, S.L., Allen, C.M., Davis, D.W., Aleinikoff, J.N., Valley, J.W., et al. 2004. Improved ^{206}Pb/^{238}U microprobe geochronology by the monitoring of a trace-element-related matrix effect: SHRIMP, ID–TIMS, ELA–ICP–MS and oxygen isotope documentation for a series of zircon standards. Chemical Geology, **205**: 115–140.

Chamberlain, K.R., Frost, C.D., and Frost, B.R. 2003. Early Archean to Mesoproterozoic evolution of the Wyoming Province: Archean origins to modern lithospheric architecture. Canadian Journal of Earth Sciences, **40**: 1357–1374.

Champion, D.C., and Sheraton, J.W. 1997. Geochemistry and Nd isotope systematics of Archaean granites of the Eastern Goldfields, Yilgarn craton, Australia: implications for crustal growth processes. Precambrian Research, **83**: 109–132.

Condie, K.C. 1993. Chemical composition and evolution of the upper continental crust: contrasting results from surface samples and shales. Chemical Geology, **104**: 1–37.

Darton, N.H. 1906. Geology of the Bighorn Mountains. US Geological Survey, Professional Paper 51. 129 pp.

Davis, W.J., and Bleeker, W. 1999. Timing of plutonism, deformation, and metamorphism in the Yellowknife Domain, Slave Province, Canada. Canadian Journal of Earth Sciences, **36**: 1169–1187.

Frost, C.D., and Fanning, C.M. 2006. Archean geochronological framework of the Bighorn Mountains, Wyoming. Canadian Journal of Earth Sciences, **43**: this issue.

Frost, C.D., Frost, B.R., Chamberlain, K.R., and Hulsebosch, T.P. 1998. The late Archean history of the Wyoming Province as recorded by granitic magmatism in the Wind River Range, Wyoming. Precambrian Research, **89**: 145–173.

Frost, B.R., Chamberlain, K.R., Swapp, S., Frost, C.D., and Hulsebosch, T.P. 2000. Late Archean structural and metamorphic history of the Wind River Range: evidence for a long-lived active margin on the Archean Wyoming craton. Geological Society of America Bulletin, **112**: 564–578.

Frost, B.R., Barnes, C.G., Collins, W.J., Arculus, R.J., Ellis, D.J., and Frost, C.D. 2001. A geochemical classification of granitic rocks. Journal of Petrology, **42**: 2033–2048.

Frost, B.R., Frost, C.D., Cornia, M., Chamberlain, K.R., and Kirkwood, R. 2006. The Teton – Wind River domain: a 2.68–2.67 Ga active margin in the western Wyoming Province. Canadian Journal of Earth Sciences, **43**: this issue.

Fruchey, B.L. 2002. Archean supracrustal sequences of contrasting origin: the Archean history of the Barlow Gap area, northern Granite Mountains, Wyoming. M.Sc. thesis, University of Wyoming, Laramie, Wyo.

Goldstein, S.L., O'Nions, R.K., and Hamilton, P.J. 1984. A Sm–Nd isotopic study of atmospheric dusts and particulates from major river systems. Earth and Planetary Science Letters, **70**: 221–236.

Gorman, A.R., Clowes, R.M., Ellis, R.M., Henstock, T.J., Spence, G.D., Keller, G.R., et al. 2002. Deep probe: imaging the roots of western North America. Canadian Journal of Earth Sciences, **39**: 375–398.

Grace, R.L.B., Chamberlain, K.R., Frost, B.R., and Frost, C.D. 2006. Tectonic histories of the Paleo- to Mesoarchean Sacawee block and Neoarchean Oregon Trail structural belt of the south-central Wyoming Province. Canadian Journal of Earth Sciences, **43**: this issue.

Gromet, L.P., and Silver, L.T. 1987. REE variations across the Peninsular Ranges Batholith: implications for batholithic petrogenesis and crustal growth in magmatic arcs. Journal of Petrology, **28**: 75–125.

Hausel, W.D. 1985. Economic geology of the Copper mountain supracrustal belt, Owl Creek Mountains, Fremont County, Wyoming. Wyoming State Geological Survey Bulletin, **28**: 1–33.

Hedge, C.E., Simmons, K.R., and Stuckless, J.S. 1986. Geochronology of an Archean granite, Owl Creek Mountains, Wyoming. US Geological Survey, Professional Paper 1388-B, pp. 27–33.

Heimlich, R.A. 1969. Reconnaissance petrology of Precambrian rocks in the Bighorn Mountains, Wyoming. University of Wyoming Contributions to Geology, **8**: 47–61.

Heimlich, R.A. 1971. Chemical data for major Precambrian rock types, Bighorn Mountains, Wyoming. University of Wyoming Contributions to Geology, **10**: 131–140.

Heimlich, R.A., and Manzer, G.K., Jr. 1973. Flow differentiation within leopard rock dikes, Bighorn Mountains, Wyoming. Earth and Planetary Science Letters, **17**: 350–356.

Heimlich, R.A., Nelson, G.C., and Malcuit, R.J. 1972. Mineralogy of Precambrian gneiss from the Bighorn Mountains, Wyoming. Geological Magazine, **109**: 215–230.

Henry, P., Stevenson, R.K., and Gariépy, C. 1998. Late Archean mantle composition and crustal growth in the western Superior Province of Canada: neodymium and lead isotopic evidence from the Wawa, Quetico, and Wabigoon subprovinces. Geochimica et Cosmochimica Acta, **62**: 143–157.

Henry, P., Stevenson, R.K., Larbi, Y., and Gariépy, C. 2000. Nd isotopic evidence for Early to late Archean (3.4–2.7 Ga) crustal growth in the western Superior Province (Ontario, Canada). Tectonophysics, **322**: 135–151.

Houston, R.S., Erslev, E.A., Frost, C.D., Karlstrom, K.E., Page, N.J., Zientek, M.L., et al. 1993. The Wyoming Province. *In* Precambrian: conterminous U.S. *Edited by* J.C. Reed, Jr., M.E. Bickford, R.S. Houston, P.K. Link, D.W. Rankin, P.K. Sims, and W.R. Van Schmus. Geological Society of America, The Geology of North America, Vol. C-2, pp. 21–170.

Jahn, B.-M., Glikson, A.Y., Peucat, J.J., and Hickman, A.H. 1981. REE geochemistry and isotopic data of Archaean silicic volcanic and granitoids from the Pilbara block, western Australia: impli-

cations for the early crustal evolution. Geochimica et Cosmochimica Acta, **45**: 1633–1652.

Johnson, K., Barnes, C.G., and Miller, C.M. 1997. Petrology, geochemistry, and genesis of high-Al tonalite and trondhjemites of the Cornucopia Stock, Blue Mountains, northeastern Oregon. Journal of Petrology, **38**: 1585–1611.

Kirkwood, R. 2000. Geology, geochronology, and economic potential of the Archean rocks in the western Owl Creek Mountains, Wyoming. M.Sc. thesis, University of Wyoming, Laramie, Wyo.

Luais, B., and Hawkesworth, C.J. 2002. Pb isotope variations in Archaean time and possible links to the sources of certain Mesozoic–Recent basalts. *In* The Earth: physical, chemical and biological development. *Edited by* C.M.R. Fowler, C.J. Ebinger, and C.J. Hawkesworth. Geological Society Special Publication (London), No. 199, pp. 105–124.

Ludwig, K.R. 1988. PBDAT for MS-DOS, A computer program for IBM PC compatibles for processing raw Pb–U–Th isotope data, version 1.04. US Geological Survey, Open-File Report 88-542.

Ludwig, K.R., and Silver, L.T. 1977. Lead-isotope inhomogeneity in Precambrian igneous K-feldspars. Geochimica et Cosmochimica Acta, **41**: 1457–1471.

Martin, H. 1987. Petrogenesis of Archaean trondhjemites, tonalites, and granodiorites from eastern Finland: major and trace element geochemistry. Journal of Petrology, **28**: 921–953.

Martin, H. 1994. The Archean grey gneisses and the genesis of continental crust. *In* Archean crustal evolution. *Edited by* K.C. Condie. Elsevier, Amsterdam, The Netherlands, pp. 205–259.

Martin, H., and Moyen, J.-F. 2002. Secular changes in tonalite–trondhjemite–granodiorite composition as markers of the progressive cooling of Earth. Geology, **30**: 319–322.

Martin, H., Chauvel, C., Jahn, B.-M., and Vidal, P. 1983. Rb–Sr and Sm–Nd ages and isotopic geochemistry of Archaean granodiorite gneisses from eastern Finland. Precambrian Research, **20**: 79–91.

Martin, H., Smithies, R.H., Rapp, R., Moyen, J.-F., and Champion, D. 2005. An overview of adakite, tonalite–trondhjemite–granodiorite (TTG), and sanukitoid: relationships and some implications for crustal evolution. Lithos, **79**: 1–24.

Mogk, D.W., Mueller, P.A., and Wooden, J.L. 1992. The nature of Archean terrane boundaries: an example from the northern Wyoming Province. Precambrian Research, **55**: 155–168.

Mueller, P.A., Peterman, Z.E., and Granath, J.W. 1985. A bimodal Archean volcanic series, Owl Creek Mountains, Wyoming. Journal of Geology, **93**: 701–712.

Mueller, P.A., Shuster, R.D., Graves, M.A., Wooden, J.L., and Bowes, D.R. 1988. Age and composition of a Late Archean magmatic complex, Beartooth Mountains, Montana–Wyoming. *In* Precambrian and Mesozoic plate margins: Montana, Idaho and Wyoming. *Edited by* S.E. Lewis and R.B. Berg. Montana Bureau of Mines and Geology, Special Publication 96, pp. 6–22.

Mueller, P.A., Wooden, J.L, and Nutman, A.P. 1992. 3.96 Ga zircons from an Archean quartzite, Beartooth Mountains, Montana. Geology, **20**: 327–330.

Mueller, P.A., Wooden, J.L., Mogk, D.W., Nutman, A.P., and Williams, I.S. 1996. Extended history of a 3.5 Ga trondhjemitic gneiss, Wyoming Province, USA: evidence from U–Pb systematics in zircon. Precambrian Research, **78**: 41–52.

Mueller, P.A., Wooden, J.L, Nutman, A.P., and Mogk, D.W. 1998. Early Archean crust in the northern Wyoming Province: evidence from U–Pb ages of detrital zircons. Precambrian Research, **91**: 295–307.

Muir, R.J., Weaver, S.D., Bradshaw, J.D., Eby, G.N., and Evans, J.A. 1995. The Cretaceous separation point batholith, New Zealand: granitoid magmas formed by melting of mafic lithosphere. Journal of the Geological Society of London, **152**: 689–701.

O'Nions, R.K., and Pankhurst, R.J. 1978. Early Archean rocks and geochemical evolution of the Earth's crust. Earth and Planetary Science Letters, **28**: 211–236.

Osterwald, F.W. 1955. Petrology of Precambrian granites in the northern Bighorn Mountains, Wyoming. Journal of Geology, **63**: 310–327.

Palmquist, J.C. 1965. Structural analysis of the Horn area, Bighorn Mountains, Wyoming. Geological Society of America Bulletin, **78**: 283–298.

Petford, N., and Atherton, M. 1996. Na-rich partial melts from newly underplated basaltic crust; the Cordillera Blanca Batholith, Peru. Journal of Petrology, **37**: 1491–1521.

Rapp, R.P., and Watson, E.B. 1995. Dehydration melting of metabasalt at 8–32 kbar: implications for continental growth and crust–mantle recycling. Journal of Petrology, **36**: 891–931.

Rapp, R.P., Shimizu, N., and Norman, M.D. 2003. Growth of early continental crust by partial melting of eclogite. Nature (London), **425**: 605–609.

Skjerlie, K.P., Patino Douce, A.E., and Johnston, A.D. 1993. Fluid absent melting of a layered crustal protolith: implications for the generation of anatectic granites. Contributions to Mineralogy and Petrology, **114**: 365–378.

Smithies, R.H. 2000. The Archaean tonalite–trondhjemite–granodiorite (TTG) series is not an analogue of Cenozoic adakite. Earth and Planetary Science Letters, **182**: 115–135.

Smithies, R.H., Champion, D.C., and Cassidy, K.F. 2003. Formation of Earth's early Archaean continental crust. Precambrian Research, **127**: 89–101.

Snelson, C.M., Henstock, T.J., Keller, G.R., Miller, K.C., and Levander, A. 1998. Crustal and uppermost mantle structure along Deep Probe seismic profile. Rocky Mountain Geology, **33**: 181–198.

Stacey, J.S., and Kramers, J.D. 1975. Approximation of terrestrial lead isotope evolution by a two-stage model. Earth and Planetary Science Letters, **26**: 207–221.

Stuckless, J.S., and Miesch, A.T. 1981. Petrogenetic modeling of a potential uranium source rock, Granite Mountains, Wyoming. US Geological Survey, Professional Paper 1225, pp. 1–34.

Stuckless, J.S., Nkomo, I.T., and Butt, K.A. 1986. Uranium–thorium–lead systematics of an Archean granite from the Owl Creek Mountains, Wyoming. US Geological Survey, Professional Paper 1388-C, pp. 39–48.

Stueber, A.W., Heimlich, R.A., and Ikramuddin, M. 1976. Rb–Sr ages of Precambrian mafic dikes, Bighorn Mountains, Wyoming. Geological Society of America Bulletin, **87**: 909–914.

Taylor, S.R., and McLennan, S.M. 1985. The continental crust: its composition and evolution. Blackwell, Oxford, UK. 312 pp.

Tilton, G.R. 1973. Isotopic lead ages of chondritic meteorites. Earth and Planetary Science Letters, **19**: 321–329.

Wakita, H., Rey, P., and Schmitt, R.A. 1971. Abundances of the 14 rare-earth elements and 12 other trace elements in Apollo 12 samples: five igneous and one breccia rocks and four soils. *In* Proceedings of the Second Lunar Science Conference, Houston, Tex., 11–14 January 1971. *Edited by* A.A. Levinson. MIT Press, Cambridge, Mass., Vol. 2, pp. 1319–1329.

Wells, R.A. 1975. Structural analysis of Precambrian rocks in the northeastern Badwater quadrangle, Wyoming. M.Sc. thesis, University of Wyoming, Laramie, Wyo.

Wells, R.A. 1977. Development of Precambrian gneiss fabric in the southern Bighorn Mountains, Wyoming. University of Wyoming Contributions to Geology, **15**: 103–117.

Whalen, J.B., Percival, J.A., McNicoll, V.J., and Longstaffe, F.J. 2002. A mainly crustal origin for tonalitic granitoid rocks, Superior

Province, Canada: implications for late Archean tectonomagmatic processes. Journal of Petrology, **43**: 1551–1570.

Wooden, J.L., and Mueller, P.A. 1988. Pb, Sr, and Nd isotopic compositions of a suite of late Archean, igneous rocks, eastern Beartooth Mountains: implications for crust–mantle evolution. Earth and Planetary Science Letters, **87**: 59–72.

Wooden, J.L., Mueller, P.A., Mogk, D.A., and Bowes, D.R. 1988. A review of the geochemistry and geochronology of Archean rocks of the Beartooth Mountains, Montana–Wyoming. *In* Precambrian and Mesozoic plate margins: Montana, Idaho and Wyoming. *Edited by* S.E. Lewis and R.B. Berg. Montana Bureau of Mines and Geology, Special Publication 96, pp. 23–42.

Zartman, R.E., and Doe, B.R. 1981. Plumbotectonics — the model. Tectonophysics, **75**: 135–162.